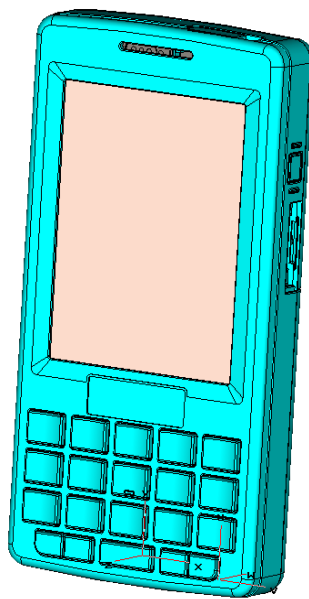


# CHALMERS



## ANTENNA DIVERSITY IN MOBILE PHONE



By  
**Bin Guo**

ANTENNA GROUP  
DEPARTMENT OF SIGNALS AND SYSTEMS  
CHALMERS UNIVERSITY OF TECHNOLOGY  
GOTHENBURG, SWEDEN  
JANUARY, 2008



Sony Ericsson



## **Abstract**

In the new generation of mobile communication systems, high data transmission rate and low bit error probability have been common requirements. However the issue of signal fading in a multi-path environment still stands as an major problem. Using antenna diversity techniques can overcome the problem. The main purpose of this thesis work is to implement receiver antenna diversity in a mobile terminal and to study the diversity performance of the diversity antenna system.

In this thesis work, simulated and measured correlation coefficient and diversity gain have been studied and compared, under the assumption of the uniform distributed propagation model. The results confirmed the equivalence of correlation coefficient calculated from far-field patterns and from S parameters. Low correlation coefficient and high diversity gain are obtained in some placements of the diversity antenna. Improvement of correlation can be obtained from the implementation of the matching networks.

## **Preface**

This report is a master thesis, completed in Antenna Group, in Sony Ericsson Mobile Communication, Kista, Sweden. The supervisor is Dr. Omid Sotoudeh, and the examiner is Prof. Per-Simon Kildal in the antenna group at Department of Signals and Systems, Chalmers University of Technology. This thesis work is performed during the period September 2007 to January 2008.

The purpose of this thesis is to implement receiver diversity antenna in mobile phone as a promising way to improve the antenna performance at the mobile terminals. This report summarizes the results of the theoretical studies, simulations and measurements of evaluating the antenna diversity performance.

## **Acknowledgements**

First of all, I would like to express my deep appreciation to my supervisor, Dr. Omid Sotoudeh, for not only giving me the opportunity to work in the Antenna Group, Sony Ericsson Mobile Communication, Kista, but also for his continued guidance, encouragement and support as a friend, throughout the whole period of the thesis.

I would also like to thank my examiner Prof. Per-Simon Kildal, for his trust and comments on both of my conference paper and thesis report.

I am very grateful to Kristina Gold, the manager of the antenna group for offering me the work opportunity and her help. Many thank to Lars Melin, who provided me with a nice apartment during the time I stayed in Stockholm and a lot of help both in life and work as always. I would like to thank Michael Moser for helping and teaching me on manufacturing prototype in relation to the measurements. I would also like to thank all the other members in antenna group for contributing to a nice working environment.

I would also very grateful to Kristian Karlsson and Prof. Jan Carlson, from SP Technical Research Institute of Sweden, it was their support and discussion that help me learn on the MPA.

Last but not least, thanks to all my friends both in Sweden and China, for their constant support and encouragement.

Bin Guo

January, 2008

## Table of contents

Abbreviations .....	8
1. Introduction.....	9
1.1 background.....	9
1.2 Purpose and method .....	9
1.3 Overview.....	10
2. Fading and Diversity.....	11
2.1 Mobile radio propagation and fading model.....	11
2.1.1 Propagation Environment .....	11
2.1.2 Fading Model .....	11
2.2 Diversity.....	12
2.2.1 Introduction.....	12
2.2.2 Diversity Achieving Mechanisms.....	13
2.2.3 Combining Techniques .....	14
2.3 Diversity Gain.....	15
2.3.1 Definition .....	15
2.3.2 Illustration of Diversity and Diversity Gain .....	16
2.3.3 Correlation Coefficient .....	17
2.3.4 Derivation of Diversity Gain .....	17
3. Study of Diversity Gain of Halve Wave Dual Dipoles.....	20
3.1 introduction .....	20
3.2 Characteristic .....	20
3.3 Correlation Coefficient .....	22
3.4 Diversity Gain.....	24
4. Study of Diversity Gain Obtained with Two PIFA Antennas on a Small Ground Plane .....	26
4.1 introduction .....	26
4.2 characteristic .....	26
4.3 Correlation Coefficient .....	29
4.4 Diversity Gain.....	31
4.5 Measurement.....	32
4.5.1 Scattered field chamber(SFC).....	32
4.5.2 Error Tolerant Analysis.....	33
4.5.2 Measurement using Network Analyzer .....	34
4.5.3 Measurement in Scattered field chamber.....	36
5. Effect of Matching Networks on Diversity Performance and Optimized in MPA.....	38
5.1 Matching Networks.....	38
5.2 Introduction of MPA.....	38
5.3 Simulation and Measurement Without Matching Network .....	41
5.4 Simulation and Measurement With Matching Network and Optimization .....	42
6. Study of Diversity Performance in Full Phone Case .....	48
6.1 Dimension selection.....	48
6.2 Unavailable Cases of Placements .....	49

6.3 Available Cases of Placements .....	52
6.4 Conclusion .....	54
7. Summary, Discussion and Future Work .....	55
Reference .....	56
Appendix A .....	57
Appendix B .....	58

## Abbreviations

<b>ADG</b>	<i>Apparent Diversity Gain</i>
<b>DA</b>	<i>Diversity Antenna</i>
<b>DG</b>	<i>Diversity Gain</i>
<b>EDG</b>	<i>Effective Diversity Gain</i>
<b>EGC</b>	<i>Equal Gain Combining</i>
<b>LOS</b>	<i>Line-Of-Sight</i>
<b>MA</b>	<i>Main Antenna</i>
<b>MPA</b>	<i>Multi Ports Antenna evaluator</i>
<b>MRC</b>	<i>Maximal Ratio Combining</i>
<b>PCB</b>	<i>Printed Circuit Board</i>
<b>SC</b>	<i>Selection Combining</i>
<b>SFC</b>	<i>Scattered Field Chamber</i>
<b>SNR</b>	<i>Signal-to-Noise Ratio</i>
<b>SWC</b>	<i>Switch Combining</i>
<b>PIFA</b>	<i>Planar Inverted F Antenna</i>
<b>UMTS</b>	<i>Universal Mobile Telecommunications System</i>



# 1. Introduction

## 1.1 background

In the new generation of mobile communication systems, high data transmission rate and low bit error probability have been common requirements. Higher performance of the mobile terminals are needed, accomplishing by increasing capacity or reducing multi-path interference. The issue of signal fading in a multi-path environment still stands as an major problem which can be overcome using antenna diversity techniques. The implementation of antenna diversity can increase the channel capacity and reduce the multi-path interference at the expense of adding extra equipment (antenna, combiner) to the receiver but no extra spectrum is consumed [1].

Two antenna functions in mobile terminals are most commonly introduced in previous works, since it can be easily implemented in real applications due to the demand of decrease of overall size of the mobile phone. In this thesis, two antennas diversity system will be studied to find the correlation coefficient of these two antennas and consequently the diversity gain which is mainly focused on in this work. Diversity gain is the most important characteristic in an antenna diversity system, and it can be obtained from correlation coefficient and embedded element efficiency [2]. When the embedded element efficiency is not taken into consideration, apparent diversity gain is obtained. Otherwise we obtain effective diversity gain, which is an absolute measure of diversity gain [3].

Another important issue is to choose proper type of antenna. PIFA antennas are chosen in this work, since they have attracted much interest due to their small size and good applicability for portable devices.

## 1.2 Purpose and method

The main purpose of this master thesis is to implement receiver diversity antenna in mobile phone as a promising way to improve the antenna performance at the mobile terminals. The diversity antenna is designed for the UMTS I Band (Rx 2112.4MHz-2167.6MHz). The studies and evaluation of the diversity performance have been conducted both in simulations and measurements. The measured results compare well with those from simulation cases using computer program. The simulation tool we used in this work is CST Micro Wave Studio, which can provide both far-field function and S parameters data for calculating the correlation coefficient of two antennas. A set of Matlab programs are developed to analyze the data from CST Micro Wave Studio for calculation of correlation coefficient and diversity gain, which is the new contribution in this work. S parameters is measured using Network Analyzer and Far field pattern is measurement in the Scattered field chamber. In this present work, three different levels of study of diversity gain are performed. Firstly, also the simplest case, two half wave dual dipoles; secondly, two PIFA antennas mounted on a small ground plane; finally, the performance of diversity antenna in a existing mobile phone prototype, Sony Ericsson M600, is studied.

### **1.3 Overview**

The theoretical part of the report consists of introduction of fading model and diversity algorithm. Those are presented in Chapter 2. In this chapter, the wave propagation environment and fading model are introduced first, and then the concept of diversity, diversity classification, and diversity algorithm are demonstrated to provide theoretical support to the analysis of diversity performance in later work.

In Chapter 3, we studied the correlation coefficient of two half wave dipoles as a function of the distance between these two dipoles in the simulation. These two dipoles are placed either parallel or orthogonal, different correlation coefficient and diversity performance are obtained from these two different cases. The simulated results are compared with those in previous works, and they are in good agreement, which verified the correctness of the settings of CST MicroWave Studio in simulation and the Matlab codes.

Then the study of two PIFA antennas mounted on a small ground plane(PCB) is presented in Chapter 4. The correlation coefficient of these two PIFA antennas, and consequently the diversity gain, are studied and developed as a function of antenna placements. The simulated and measured results are compared and shown together in this chapter.

The main focus in chapter 5 is on matching networks and their effects on diversity gain. Tests are done in simulation on simple antenna matching networks in order to improve diversity performance. Furthermore the matching networks are optimized using MPA [4], which is developed by SP Technical Research Institute of Sweden, to get low correlation coefficient and high diversity gain. Then the prototypes are measured and compared with simulated results.

In Chapter 6, we are concerned with the diversity performance in full phone case. Several simulation cases of different placements of diversity antenna have been done in order to put another antenna inside an existing phone, Sony Ericsson M600, with the purpose of studying the performance of both antennas, main antenna and diversity antenna.

In the end, summary is concluded and leads to future work.

## 2. Fading and Diversity

### 2.1 Mobile radio propagation and fading model

#### 2.1.1 Propagation Environment

The propagation mechanism of radio waves in a mobile environment is a vital aspect in modern wireless communication systems. Since the transmission paths between the transmitter and the receiver vary from simple line-of-sight (LOS) to one that is obstructed by buildings, mountains and so on, the radio channels are extremely random and unpredictable.

Shadowing and fading are the most important phenomena which cause significant impairment to the quality of a mobile radio channel. The strengths of the waves decrease at the distance between the transmitter and receiver increases and this is called shadowing or large-scale fading (also called long-term fading); on the other hand, small-scale fading (also called short-term fading) characterizes the rapid fluctuations of the received signal strength over very short travel distances or short time durations.

Figure 2.1 illustrates log-normal shadowing according to log-distance path loss model [5] and Rayleigh fading.

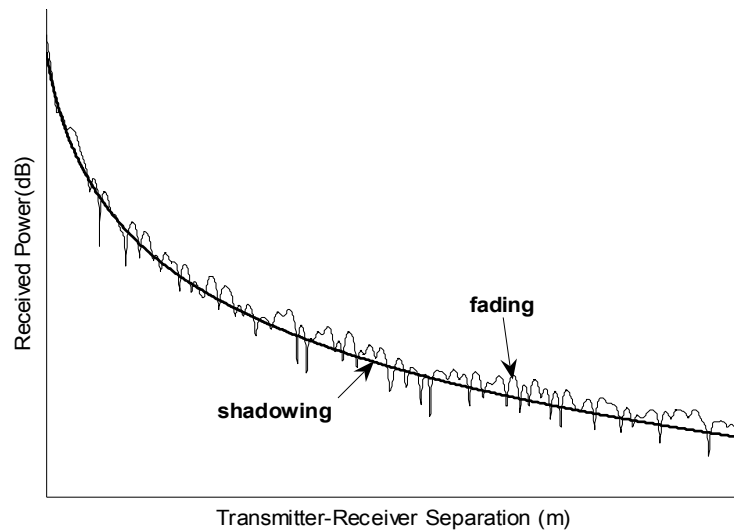


Figure 2.1 illustration of shadowing and fading

#### 2.1.2 Fading Model

In this thesis, small-scale fading, or simply fading, will be focused on. Since fading is used to describe the performance of the received signal during a short period, the large-scale path loss effects might be ignored. The fading is caused by multi-path, which means

two or more versions of the transmitted signal arriving at the receiver at slightly different times, in the radio channel. These different versions of received signals are created by the reflections and diffractions from local objects which block the line-of-sight (LOS) signal between the transmitter and receiver. In the receiver the different versions of signals are added, either constructively or destructively, and create a received signal which may varies rapidly in both amplitude and phase, depending on the local objects and speed of the receiver. Thus when the different signals add destructively, the received signal is likely to suffer sudden dips which are unexpected and will degraded the performance of the channels, shown in Figure 2.2.

When there is no line-of-sight (LOS) path between transmitter and receiver, the received signal will perform a Rayleigh fading [6]. That means the envelope of the received signal is Rayleigh distributed at every point in time. Figure 2.2 shows a Rayleigh distributed signal envelope as a function of time.

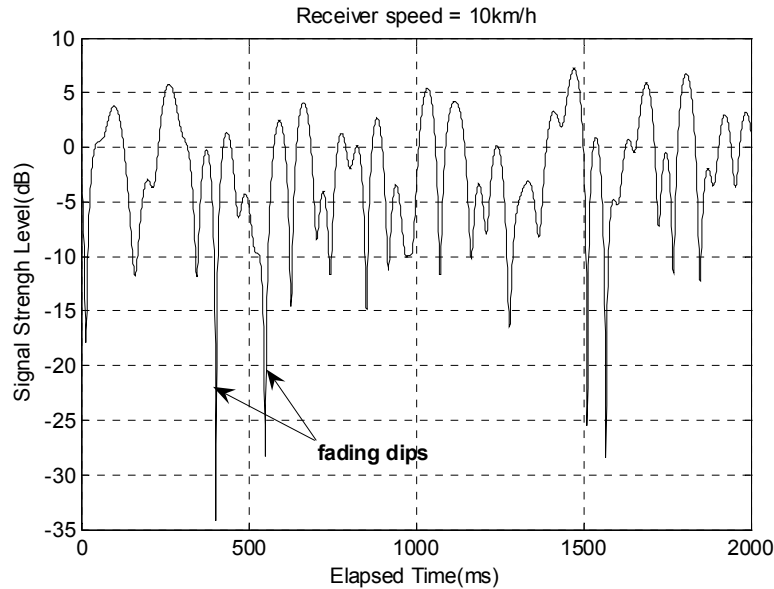


Figure 2.2 A typical Rayleigh fading envelope at 2.1 GHz (simulated in MATLAB)

## 2.2 Diversity

### 2.2.1 Introduction

The major cause of the poor performance on fading channels is the occasional fading dips, even at high average SNRs, there is a significant probability that fading dips occur. To overcome the effect of fading dips, diversity techniques are introduced.

Usually the diversity is applied in receiver site providing wireless link improvement at relatively low cost. The key idea of diversity is artificially creating several independent replicas of the original path. If one path undergoes a deep fade, another independent path may have a strong signal. By having more than one path to select from under some selection schemes, both the instantaneous and average SNRs at the receiver may be

improved. Each path or channel is called a diversity *branch*. Figure 2.3 shows a general block diagram of antenna diversity scheme.

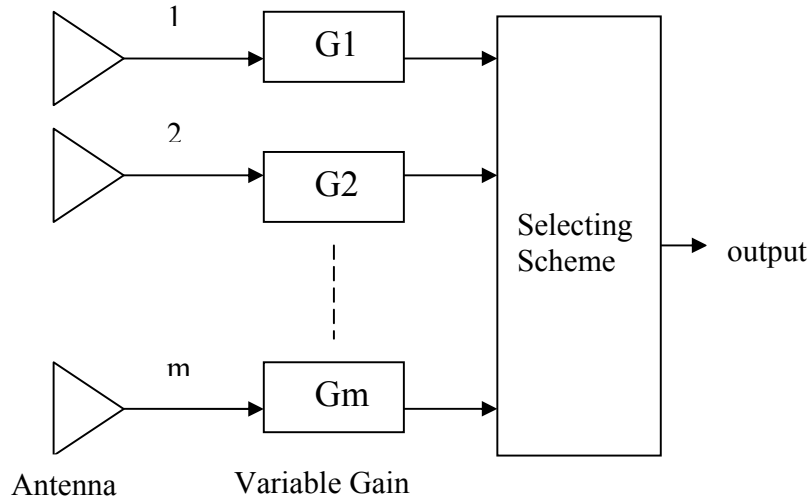


Figure 2.3. Generalized diagram for antenna diversity

## 2.2.2 Diversity Achieving Mechanisms

### Micro-diversity and macro-diversity

According to the two different types of fading, small-scale fading and large-scale fading, two corresponding diversity techniques are implemented. In order to prevent deep fades from occurring, *microscopic diversity techniques* is applied to mitigate small-scale fading effects by selecting the optimized signal all the time. *Microscopic diversity* is also called *antenna diversity* [5]. On the other hand, *macroscopic diversity techniques* is applied in the case of large-scale fading to improve the average SNR on the forward link by selecting a base station which is not shadowed when others are. In this work, antenna diversity in mobile phone will be studied, and *macroscopic diversity* will not be addressed here.

Diversity can be created by many means. The following is a brief introduction of some of them, in which Space diversity, Polarization diversity and Pattern diversity can be utilized in antenna systems.

- Space diversity

Space diversity is the most common and simple diversity scheme used in wireless communication. In antenna system, two or more antennas are set apart with considerable distance.

- Time diversity

Time diversity has been particularly applied in digital data transmission. In time diversity, the information bits are repeatedly transmitted at time intervals that exceed the coherence time of the channel, so that multiple repetitions will undergo independent fading conditions, when they are received and combined, diversity can be obtained, [5] and [7].

- Frequency diversity

Frequency diversity is implemented by transmitting information on more than one carrier frequency. The same signal at sufficiently spaced carrier frequencies will provide independently fading versions of the signal, thus the probability of simultaneous fading of combined signal at the receiver will be very low [5] and [7].

- Polarization diversity

Two polarizations, vertical and horizontal, from two antennas can carry two signals on one radio frequency over wireless links. Polarization diversity can be exploited by using orthogonal polarization. Polarization diversity is typically used in fixed radio links which vary slowly in time.

There are several other types of diversity scheme, such as Pattern diversity, energy diversity, directional diversity and so on, which can be found more in detail in [5] and [7]. In this thesis, space diversity is utilized. Because space diversity is the simplest diversity scheme to implement as mentioned above, especially in mobile phone.

### 2.2.3 Combining Techniques

#### Selection Combining (SC) and Switch Combining (SWC)

Selection combining and switch combining are very similar and simplest methods to implement. In selection combining, the strongest signal is selected at the receiver from M received signal branches. In Switch Combining, the channel with highest instantaneous SNR  $\gamma_i$  ( $i = 1, 2, \dots, m$ , the branch number) will be chosen. There is a threshold SNR value  $\Gamma$ . The receiver choose a channel as long as its  $\gamma_i > \Gamma$ ; when  $\gamma_i$  fall below the threshold  $\Gamma$ , then the receiver scan for a new diversity branch with  $\gamma_i > \Gamma$ .

#### Maximal Ratio Combining (MRC)

In this method, the signals from all of the M branches are weighted according to their individual signal to noise power ratio and then summed. The MRC is optimum in the sense that it is based on the weighted summed signal not only one signal selected from one branch. The SNR out of the MRC combiner is simply the sum of the SNRs in each branch [5], thus it has the advantage of producing an output with an acceptable SNR even when none of the individual signals themselves are acceptable. MRC gives the best

performance to overcome the fading problem, but often at much greater cost and complexity than other diversity techniques.

### Equal Gain Combining (EGC)

EGC can be seen as simplified version of MRC, in this method, all the branch weights are set to unity, but the signals from each branch are co-phased and combined at the receiver.

Among the MRC, EGC, SC, the performance of MRC is the best but the equipment is complicated. The performance of SC is lower than that of MRC and EGC, but the equipment is simple to build, which is important to utilize in mobile phone. Since the dimension of the mobile phone become smaller and smaller as a trend of modern mobile phone design, it is more important for components easy to implement inside the mobile phone. Furthermore, since the computation complexity will be increased using MRC but not much more diversity gain would be obtained; SC is usually chosen as the diversity scheme. That is the reason why SC is chosen as the combining technique in this work.

## 2.3 Diversity Gain

### 2.3.1 Definition

In 2.2, diversity scheme and combining methods are introduced. Diversity combining means that two antennas are used together to receive a signal, and that we combine the replicas of the received signals in a desirable manner to improve the performance. In antenna system, there are mainly three kinds of diversity, space diversity (locating the antennas away from each other), polarization diversity (using orthogonally polarized antennas) and pattern diversity (using different radiation patterns).

Diversity gain is the most important characteristic of the diversity system. In general, the diversity gain is the difference between the combined CDF (Cumulative Distribution Function) and a reference CDF at a certain CDF-level, normally chosen to be 1%. There are three main definitions on diversity gain distinguished by different reference CDF [8]. **Apparent diversity gain**, the reference CDF is that of strongest average signal level; **effective diversity gain**, the reference CDF is that of an ideal single antenna which means 100% radiation efficiency; **actual diversity gain**, the reference CDF is that of the exiting practical single antenna which is to be replaced by the diversity antenna.

Normally, we refer to apparent diversity gain when we talk about diversity gain. The diversity gain can be expressed as

$$G_{div} = \frac{P_{div}}{P_{branch}} \quad (2-1)$$

In which  $P_{div}$  is the power level after diversity combining, and  $P_{branch}$  is the power level of the reference branch. Both power levels must be read at the same CDF level. The effective diversity gain can be expressed as

$$G_{effdiv} = \frac{P_{div}}{P_{ideal}} = \frac{P_{div}}{P_{branch}} \cdot (e_{rad eff})_{branch} \quad (2-2)$$

where  $P_{ideal}$  is the power level of ideal single antenna with 100% radiation efficiency, and  $(e_{rad eff})_{branch}$  means the radiation efficiency of the reference branch.

### 2.3.2 Illustration of Diversity and Diversity Gain

As mention in 2.1, the received signal power level in a multi-path environment with no line of sight is statistically distributed as a Rayleigh function. Consider M independent Rayleigh fading channels available at the receiver. Assume that each branch has the same mean SNR  $\Gamma$ . For selective combining scheme, the probability that all M independent diversity branches receive signals which are simultaneously less than some specific SNR threshold  $x$  is [5]

$$\Pr(\gamma_1, \gamma_2 \dots \gamma_M < x) = (1 - e^{-\frac{x}{\Gamma}})^M \quad (2-3)$$

Hence, the probability that instantaneous combiner output SNR  $\gamma$  is below to some value  $x$  is

$$\Pr(\gamma < x) = (1 - e^{-\frac{x}{\Gamma}})^M \quad (2-4)$$

From which, Figure 2.4 was plotted to show the probability distributions of relative SNR threshold for M branch selection diversity. The concept of Diversity Gain is also illustrated in this graph(at 1% probability).

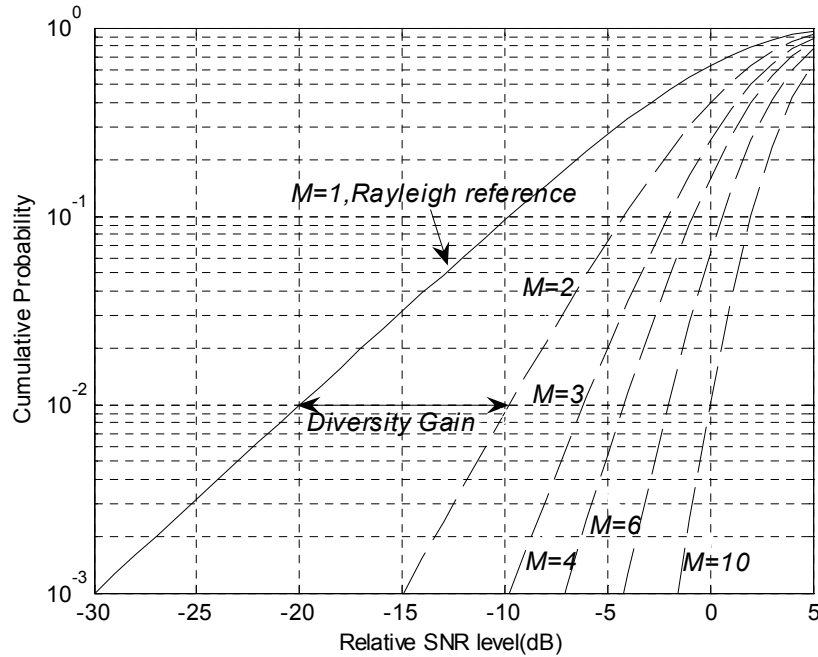


Figure 2.4. Graph of probability distributions of relative SNR threshold for M branch selection diversity in ideal case.



### 2.3.3 Correlation Coefficient

The correlation coefficient  $\rho$  between received signals on two ports can be calculated from the correlation between the induced voltages in the received equivalent circuits of the two ports. The voltages express can be readily transformed to deterministic integrals in terms of the normalized coupling between the far field functions of the two ports [9]:

$$\rho = \frac{\iint_{4\pi} \bar{G}_{1total} \bar{G}_{2total}^* d\Omega}{\sqrt{\iint_{4\pi} \bar{G}_{1total} \bar{G}_{1total}^* d\Omega \iint_{4\pi} \bar{G}_{2total} \bar{G}_{2total}^* d\Omega}} \quad (2-5)$$

In which  $\bar{G}_{1total}$   $\bar{G}_{2total}$  are the far-field functions of each of the separated antennas.  $\bar{G}_i = G_\theta \hat{\theta} + G_\phi \hat{\phi}$  ( $i = 1, 2$ ),  $G_\theta$  and  $G_\phi$  are the components in the direction of  $\hat{\theta}$  and  $\hat{\phi}$ , respectively. In the simulation, one antenna is excited and the other is terminated by 50 Ohm impedance, and the two antennas are located parallel and the distance between them is  $d$ . The correlation coefficient will be changed as  $d$  is changing, since the coupling between two dipoles depends on the distance between these two dipoles.

Another approach to compute the envelope correlation coefficient from the S-parameter characteristic of the antenna system has been derived in [10]. It shows that in some simple case of environment, such as uniform random field case, the correlation coefficient can be calculated from S-parameters. The envelope correlation coefficient in terms of the S-parameter of the antenna system can be expressed as:

$$\rho_e = \frac{|S_{11}^* S_{12} + S_{21}^* S_{22}|^2}{(1 - (|S_{11}|^2 + |S_{21}|^2))(1 - (|S_{22}|^2 + |S_{12}|^2))} \quad (2-6)$$

In this way, the correlation coefficient can be calculated more efficiently. The relation between the complex cross correlation coefficient  $\rho$  and the envelope correlation coefficient  $\rho_e$  is demonstrated in [1]:

$$|\rho|^2 \approx \rho_e \quad (2-7)$$

In this work, both methods for calculating the correlation coefficient are utilized.

### 2.3.4 Derivation of Diversity Gain

It is worth to note that the diversity gain can be calculated from the cumulative probability and compared with the reference. In a diversity antenna system, the antennas are not ideally uncorrelated, hence the correlation between two antennas always exists. The cumulative probability that the instantaneous combiner output SNR  $\gamma$  is below to some value  $x$  has been derived in [7]. The result is written in either of the two equivalent forms,

$$\Pr(\gamma < x) = 1 - \exp\left(-\frac{x}{\Gamma_1}\right)Q\left(\sqrt{\frac{2x}{\Gamma_2(1-|\rho|^2)}}, |\rho| \sqrt{\frac{2x}{\Gamma_1(1-|\rho|^2)}}\right) - \exp\left(-\frac{x}{\Gamma_2}\right) \quad (2-8)$$

$$\begin{aligned} & [1 - Q\left(|\rho| \sqrt{\frac{2x}{\Gamma_2(1-|\rho|^2)}}, \sqrt{\frac{2x}{\Gamma_1(1-|\rho|^2)}}\right)] \\ & = 1 - \exp\left(-\frac{x}{\Gamma_1}\right)Q\left(\sqrt{\frac{2x}{\Gamma_2(1-|\rho|^2)}}, |\rho| \sqrt{\frac{2x}{\Gamma_1(1-|\rho|^2)}}\right) \\ & - \exp\left(-\frac{x}{\Gamma_2}\right)Q\left(\sqrt{\frac{2x}{\Gamma_1(1-|\rho|^2)}}, |\rho| \sqrt{\frac{2x}{\Gamma_2(1-|\rho|^2)}}\right) \quad (2-9) \\ & + \exp\left[-\frac{x}{1-|\rho|^2}\left(\frac{1}{\Gamma_1} + \frac{1}{\Gamma_2}\right)\right]I_0\left[\frac{2|\rho|x}{(1-|\rho|^2)\sqrt{\Gamma_1\Gamma_2}}\right] \end{aligned}$$

In which,  $\Gamma_1$   $\Gamma_2$  are the mean SNR for antenna 1 and antenna 2 in the diversity antenna system, respectively. The Q function is the Marcum function.  $I_0$  is the modified zero order Bessel function of first kind.  $\rho$  is the complex cross correlation coefficient.

The conditions for achieving good diversity gain are illustrated below: the correlation coefficient between branch signals should be zero or 'low', and the mean SNR's in each branch should be 'similar'[1]. An assumption thus has been made that  $\Gamma_1$   $\Gamma_2$  are set equal to fulfill the condition, let's say  $\Gamma$ , for mean SNR of both antennas. From the assumption, the formulas (2-8) (2-9) become

$$\begin{aligned} \Pr(\gamma < x) & = 1 - \exp\left(-\frac{x}{\Gamma}\right)[1 - Q\left(|\rho| \sqrt{\frac{2x}{\Gamma(1-|\rho|^2)}}, \sqrt{\frac{2x}{\Gamma(1-|\rho|^2)}}\right) \\ & + Q\left(\sqrt{\frac{2x}{\Gamma(1-|\rho|^2)}}, |\rho| \sqrt{\frac{2x}{\Gamma(1-|\rho|^2)}}\right)] \quad (2-10) \end{aligned}$$

$$\begin{aligned} & = 1 - 2 \exp\left(-\frac{x}{\Gamma}\right)Q\left(|\rho| \sqrt{\frac{2x}{\Gamma(1-|\rho|^2)}}, \sqrt{\frac{2x}{\Gamma(1-|\rho|^2)}}\right) \quad (2-11) \\ & + \exp\left[-\frac{2x}{\Gamma(1-|\rho|^2)}\right]I_0\left[-\frac{2|\rho|x}{\Gamma(1-|\rho|^2)}\right] \end{aligned}$$

From which, the cumulative probability as a function of relative SNR at a certain correlation coefficient value can be calculated. According to a certain level (for instance, 1%) of cumulative probability and comparing with the reference, diversity gain can be obtained.

There is another approximate approach to obtain diversity gain. The relation between diversity gain and correlation coefficient can be also approximately given by the following approximate formula [11]:

$$G_{app} = 10 \cdot e_p \quad \text{with } e_p = \sqrt{1-|\rho|^2} \quad (2-12)$$

where  $G_{app}$  is the apparent diversity gain, 10 is the maximum apparent diversity gain<sup>1</sup> at 1% CDF level using selection combining.  $e_p$  is the correlation efficiency, also known as the reduction in diversity gain due to correlation coefficient. If the correlation close to unity,  $\rho$  is scaled with a factor 0.99, and the formula(2-12) becomes [11]

$$e_p = \sqrt{1 - |0.99 \cdot \rho|^2} \quad (2-13)$$

The effective diversity gain can be defined as following formula

$$G_{eff} = e_{rad} \cdot G_{app} \quad (2-14)$$

In which,  $G_{app}$  is the apparent diversity gain, and  $e_{rad}$  is the embedded element efficiency [6].

Figure 2.5. shows the relation between correlation coefficient and diversity gain using selection combining scheme. Generally, the lower correlation coefficient is, the larger diversity gain can be obtained. Furthermore, and the diversity gain is close to 10.2 dB which is the theoretical value when two channels are uncorrelated (correlation coefficient is 0). It is worth to point out that when the correlation coefficient is reduced to around 0.5, high diversity gain, around 9.5 dB, could still be obtained. However, according to the graph, less and less additional diversity gain can be obtained, if the correlation coefficient is reduced from 0.5 to 0.

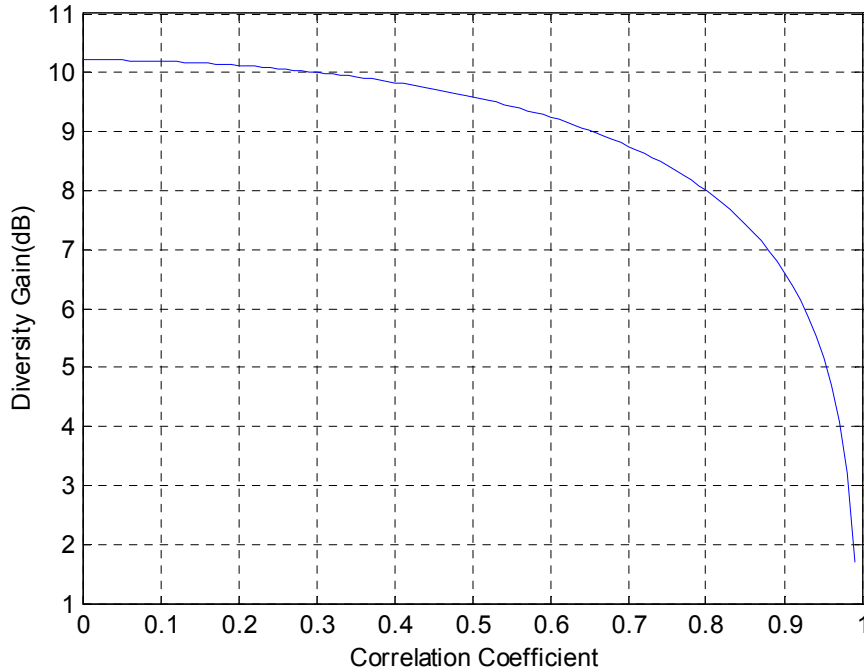


Figure 2.5. Diversity gain against correlation coefficient (selection combining).

<sup>1</sup>. 10.46 or 10.2dB is more accurate in this work according to the result from MATLAB simulation.

### 3. Study of Diversity Gain of Halve Wave Dual Dipoles

#### 3.1 introduction

Dipole antennas are wired antennas excited from the center of the wire. These antennas are the simplest practical antennas from a theoretical point of view. Therefore, study of dipoles was done first in this work. Typically a dipole antenna is formed by two quarter wavelength conductors or elements placed back to back for a total length of  $\frac{\lambda}{2}$ . A standing wave on an element of a length  $\frac{\lambda}{4}$  yields the greatest voltage differential, as one end of the element is at a node while the other is at an antinode of the wave, showed in Figure 3.1.

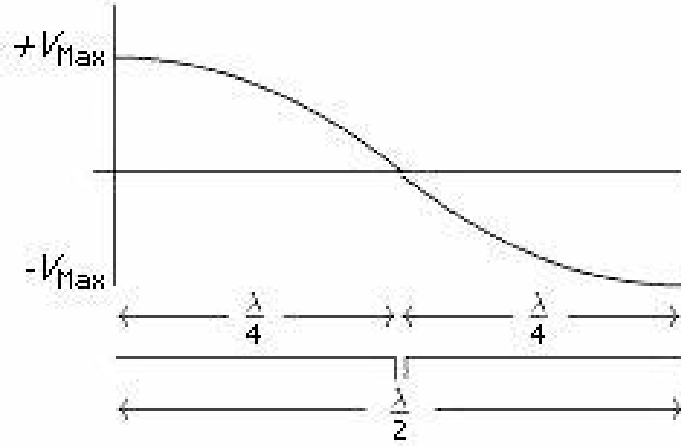


Figure 3.1. illustration of  $\frac{\lambda}{2}$  dipole

In this work, UMTS I Rx Band (2.12GHz-2.17GHz) will be concentrated; the central frequency is 2.1 GHz. In this case,  $\frac{\lambda}{2}$  length dipole is 35.7mm.

#### 3.2 Characteristic

In the simulation, two cases are defined as following to learn the characteristic of dual dipoles: two dipoles are located in the free space parallel or orthogonal, respectively, and the distance between two dipoles is set 50mm in both cases. Figure 3.2. illustrates the two different geometries, one is parallel and the other one is orthogonal.

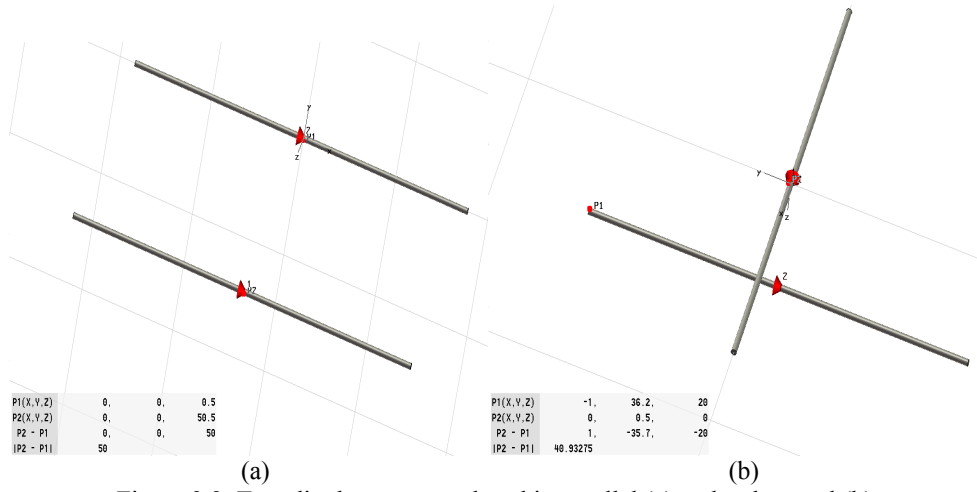


Figure 3.2. Two dipole antennas placed in parallel (a) and orthogonal (b).

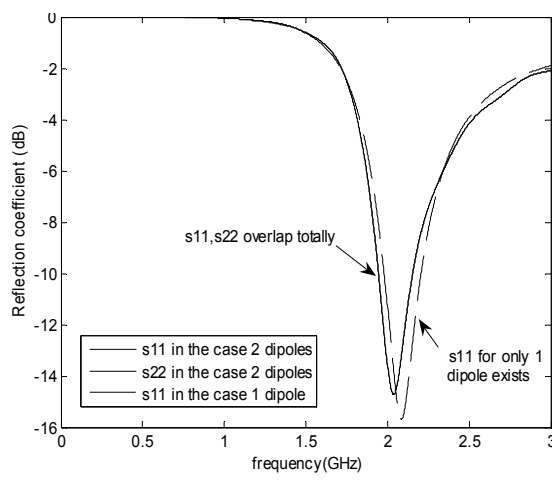


Figure 3.3. Comparison of reflection coefficient between one dipole and two parallel dipoles

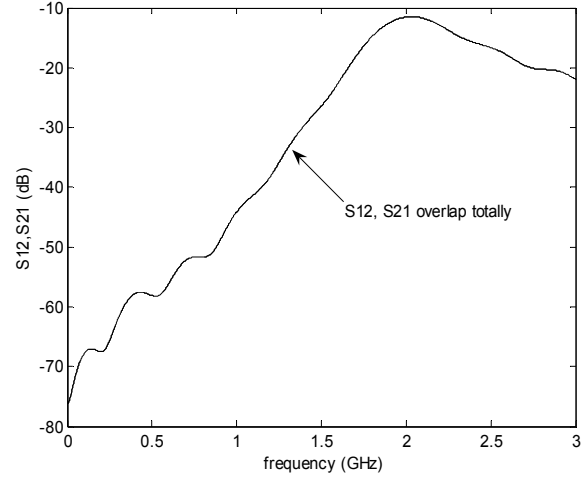


Figure 3.4. Comparison of S12 of the two dipoles

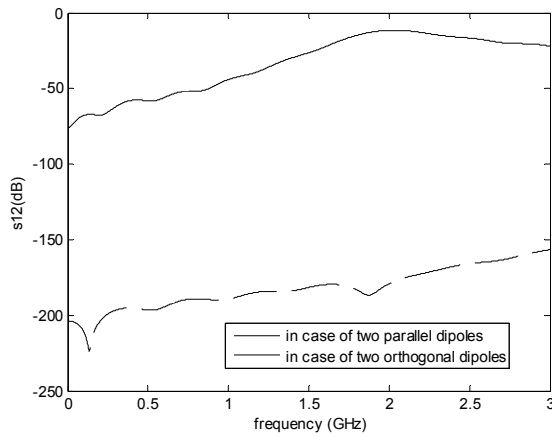


Figure 3.5. Comparison of S12 between two different geometries of two dipoles

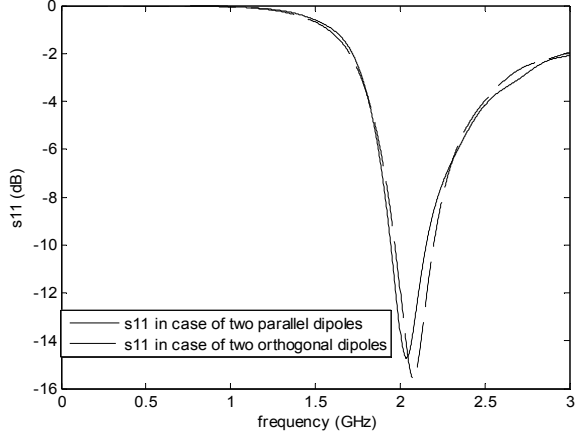


Figure 3.6. Comparison of S11 between two different geometries of two dipoles

In Figure 3.3, the reflection coefficient of one dipole and two parallel dipoles are plotted together, it is seen that the resonant frequency will shift left slightly when two dipoles are

considered in a same antenna system. This is due to mutual coupling between the two dipoles. Figure 3.4 illustrate the mutual coupling(S12) when two dipoles are parallel, the value of S12 is below -10dB, In Figure 3.5, the mutual couplings of two dipoles both in case of parallel and orthogonal are compared in the same graph. When two dipoles are orthogonal, the mutual coupling becomes nearly zero. Figure 3.6 shows the difference of the resonant frequency between the case of parallel and orthogonal. It is worth to point out that the curve of reflection coefficient (S11) in the case of orthogonal is almost the same as that of single dipole if we compare Figure 3.6 and Figure 3.3. The reason is again due to the negligible coupling. But in parallel case, the effect from another antenna has to be considered, that is why the resonant frequency in parallel case is effected.

### 3.3 Correlation Coefficient

To calculate the correlation coefficient, both of two cases, parallel and orthogonal, are taken into consideration. In each case, we consider two sub-cases, designed length and optimized length<sup>2</sup> of dipoles. The half-wave dipoles are designed for 2.1GHz, the calculated length for this frequency is called designed length. However, the resonant frequency is not at 2.1 GHz accurately if using dipoles of designed length. Hence the length of dipoles are adjusted to meet the requirement of resonant frequency. The adjusted dipoles' length is named optimized length in this work. In the simulation, the main purpose is to study the relation of correlation coefficient and the spacing distance between two dipoles.

**Case1.** Two parallel dipoles of different length (designed length  $\frac{\lambda}{2}$  and optimized length)

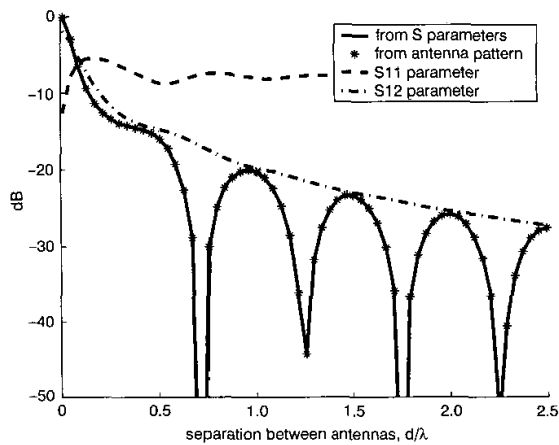


Figure 3.7. Envelope correlation and S-parameters for two half-wave dipoles against their separation [6].

Figure 3.7 is from [10], the results obtained by both methods are shown the spacing between two dipoles. It is clearly seen that both methods provide the same result, it is also interesting to note that mutual coupling alone does not provide a good estimate for the envelope correlation.

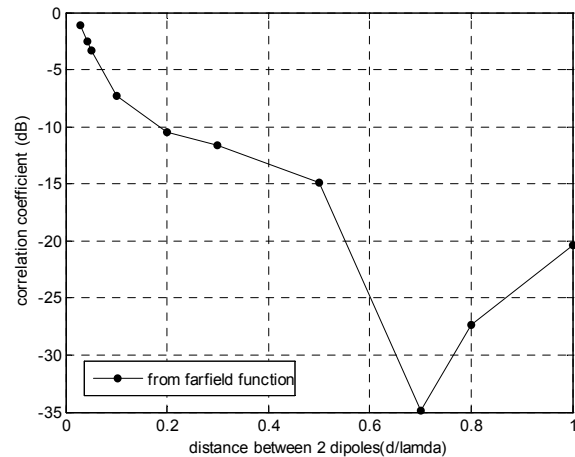


Figure 3.8. Envelope correlation calculated using data from MWS.

<sup>2</sup> In this work, designed length is 35.7mm; optimized length is 31.5mm.

Figure 3.8 shows envelope correlation coefficient results obtained by simulating in CST and calculating using far-field function. The result shown on Figure 3.8 agrees with that of Figure 3.7 well.

The S parameters of  $\frac{\lambda}{2}$  length of two parallel dipoles are shown on Figure 3.9.

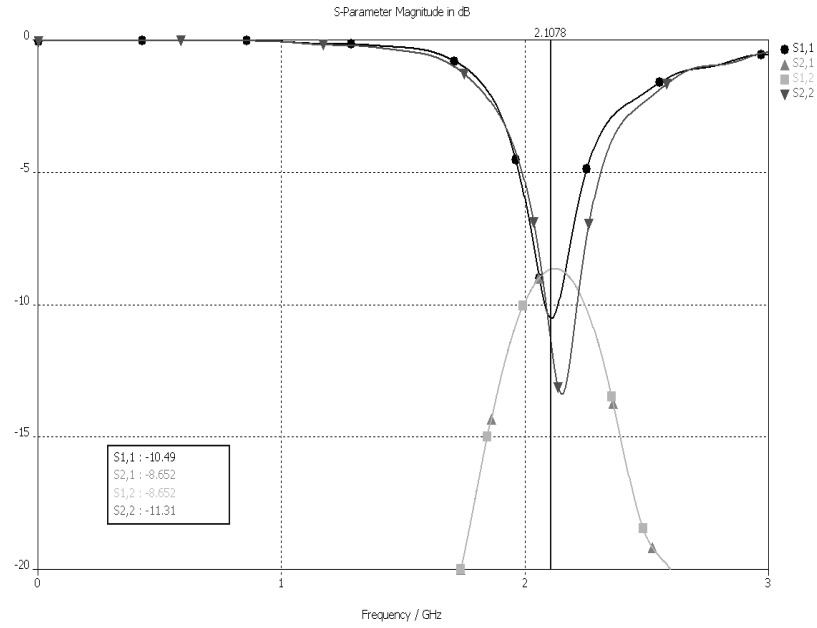


Figure 3.9 S parameters of two parallel  $\frac{\lambda}{2}$  dipoles

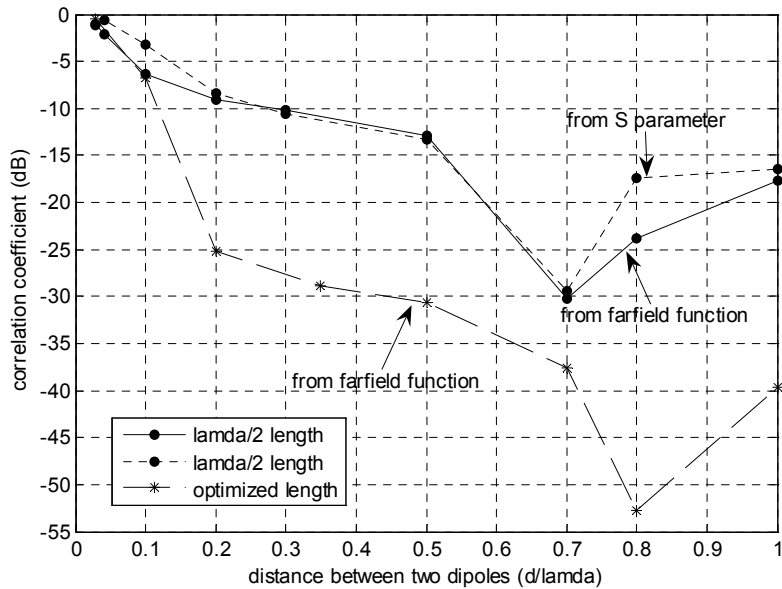


Figure 3.10. Envelope correlation using both far-field and S parameters methods

The envelope correlation coefficient calculated from far-field function and from S parameters are compared in Figure 3.10, also the comparison between  $\frac{\lambda}{2}$  length and optimized length are shown on the same Figure. From Figure 3.10, it is easily obtained that the result from far-field function and that of S parameter agree well.

From Figure 3.10, the correlation coefficient firstly decreases as the distance between two dipoles increases, and lowest correlation coefficient occurs when the distance is  $0.7 \lambda$ . If the distance is continuously increased from  $0.7 \lambda$ , the correlation coefficient will slightly increase.

**Case 2.** Two orthogonal dipoles of different length (designed length and optimized length)

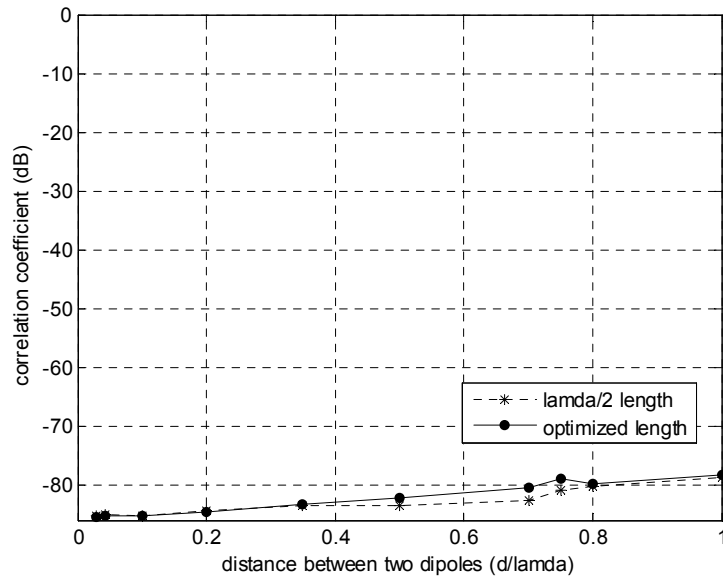


Figure 3.11. Comparison of Envelope correlation coefficient between  $\frac{\lambda}{2}$  and optimized length

Figure 3.11. shows the comparison of envelope correlation between  $\frac{\lambda}{2}$  and optimized length, both using far filed function. From the results obtained from the simulation, the correlation coefficient between two orthogonal dipoles is nearly zero. That means the orthogonal dipoles are uncorrelated, which agree with the theoretical value.

### 3.4 Diversity Gain

From the formula mentioned in Chapter 2, diversity gain of dipoles can be calculated from correlation coefficient. All the data is from MWS and one dipole case is regarded as the reference, the curve of which is the same as the Rayleigh curve theoretically.



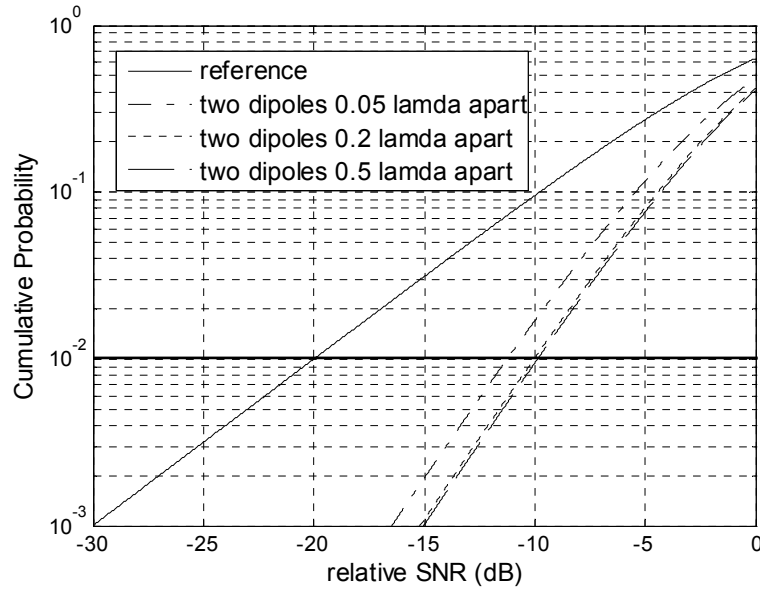


Figure 3.12. Cumulative probability density function of two parallel  $\frac{\lambda}{2}$  dipoles.

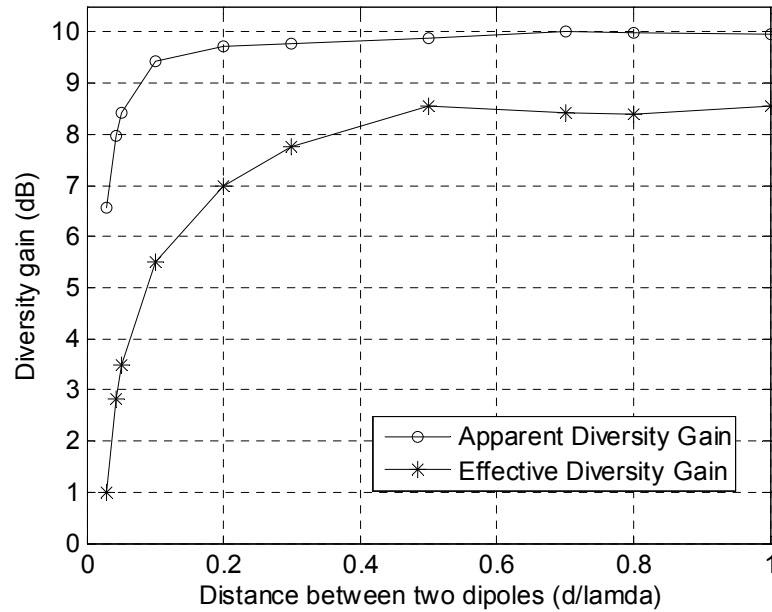


Figure 3.13. Diversity Gain against distance of two parallel  $\frac{\lambda}{2}$  dipoles.

Figure 3.12 shows the cumulative probability against relative SNR when the dipoles are separated by different spacing. Compared with Figure 2.4, it is obtained that when the two dipoles are located far away from each other, the curve will approach to the curve of two theoretical branches. Furthermore, the diversity gain can be read from the curve directly at 1% probability. Both apparent diversity gain and effective diversity gain against different distance between two dipoles are plotted together in Figure 3.13, from which an interesting result is obtained that the diversity gain does not increase linearly following the growth of the distance. When the two dipoles are  $0.2 \lambda$  apart from each other, little additional diversity gain can be obtained.

## 4. Study of Diversity Gain Obtained with Two PIFA Antennas on a Small Ground Plane

### 4.1 introduction

PIFA is the abbreviation of Planar-Inverted-F-Antenna. PIFA antennas are commonly used in the mobile terminals. The PIFA is basically a modification of the inverted F antenna (IFA) consisting of a short vertical monopole wire. To increase the bandwidth a modification is made by replacing the wires with a horizontal plate and a vertical short circuit plate.

Conventional PIFA comprise of a top patch, a shorting pin and a feeding pin.

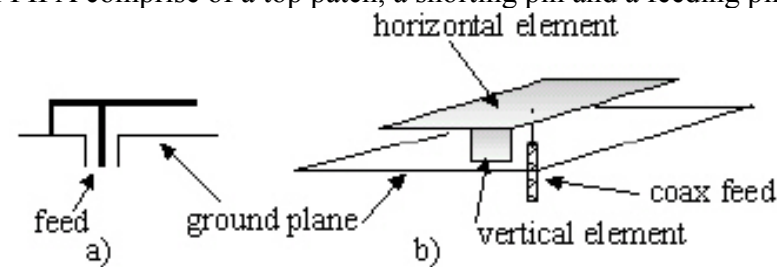


Figure 4.1. Illustration of PIFA antenna

The top patch is mounted above a ground plane; the ground pin and feeding pin, connected at proper positions to the top patch, have the same length as the distance between the top patch and the ground plane. Figure 4.1 shows the illustration of PIFA antenna. Placing L-shaped, U-shaped slits or other shaped slits (normally meandering techniques) in the main resonating patch produces dual frequency operation. Upper bound of the frequency is controlled by the length and width of the slit, and the lower resonant frequency is controlled by the length and width of the main patch.

PIFA antenna has advantages due to the minimum occupied volume with regard to portability and overall size minimization of the mobile terminal and shape.

### 4.2 characteristic

A PIFA antenna was designed as shown in Figure 4.2 and simulated in order to study the characteristic of PIFA antennas. The dimension of the ground is  $100 \times 50 \text{ mm}^2$ , which is the same as the standard stick type phone models.

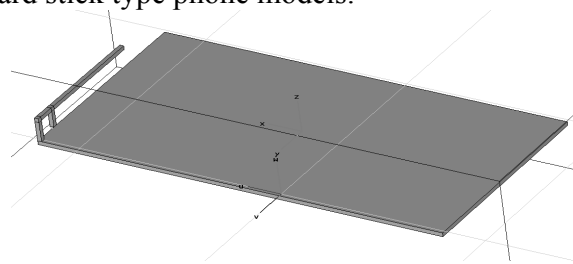


Figure 4.2. Geometry of one PIFA antenna mounted on PCB

Mainly three parameters in this case have effect on the performance of S parameters: the length(L), the height(h), and the distance(dv) between the feeding point and the ground point. These parameters are changed to observe different performances of the return loss(S11) of the designed PIFA antenna. All the result are plotted in Figure 4.3. The main purpose is to find a better performance at a certain resonant frequency.

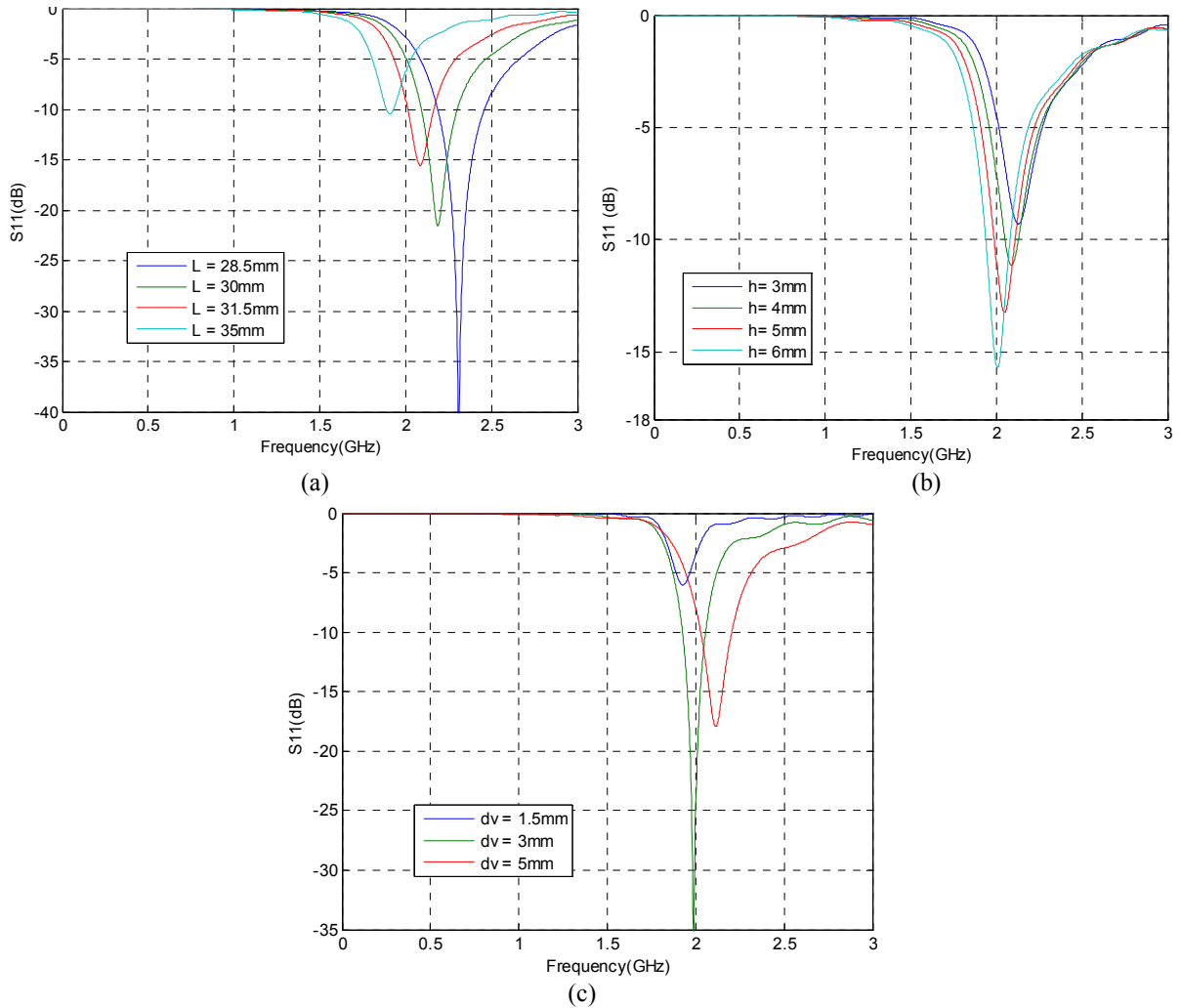


Figure 4.3.  $S_{11}$  as a function of frequency and dimension parameters. (a) length.(b) height. (c) distance between the feeding point and the ground point.

Figure 4.3(a) shows the effect of changing length (L) on  $S_{11}$  when other parameters(height, distance) are set at a certain value. The resonant frequency will shift right in the graph, which means the resonant frequency increases, when the length decreases. Furthermore less return loss can be obtained as the PIFA antenna becomes shorter. Figure 4.3(b) shows the effect of changing height (h) on  $S_{11}$  when other parameters (length, distance) are set at a certain value. When the height is increased, the resonant frequency will decrease and less return loss can be obtained. Figure4.3(c) shows the effect of changing the distance (dv) between feeding point and ground point on  $S_{11}$

when other parameters (length, height) remain unchanged. When the feeding point is further away from the ground point, higher resonant frequency is obtained. More details about the relation between distance and return loss will be illustrated on Smith Chart in Figure 4.4.

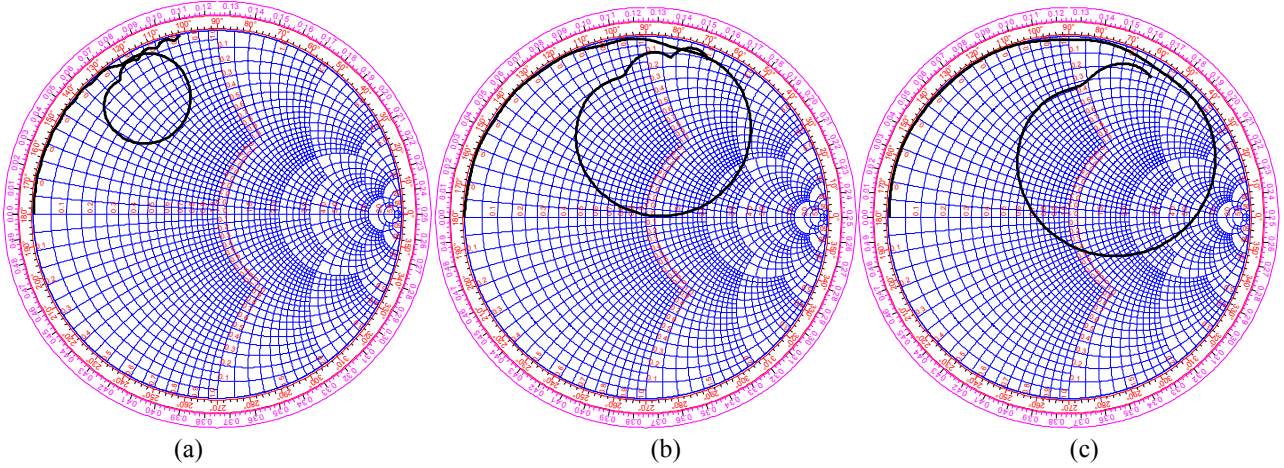


Figure 4.4 Typical feed positions and return loss plots for a PIFA : (a)  $dv = 1.5\text{mm}$ , under-coupled; (b)  $dv = 3\text{mm}$ , critically coupled; (c)  $dv = 5\text{mm}$ , over-coupled.

If the feed point is close to the ground point the  $S_{11}$  has the characteristic behavior shown in Figure 4.4(a). The  $S_{11}$  plot remains close to the edge of the Smith Chart at most frequencies, with a small circle at the frequency at which the antenna is resonant. This is referred to as an under-coupled response. As the feed point is moved away from the ground point, the size of the circle indicating the resonant frequency grows until at some point it passes through the center of the Smith Chart ( $50 + j0$  ohms), this situation is referred to as critical coupling (Figure 4.4(b)). As the feed point is moved further away from the ground point the size of the resonant circle continues to grow, as in Figure 4.4(c), this state is called over-coupled [12].

Furthermore, two PIFA antennas were built in the simulation to study the influence of return loss on each other and the coupling between them. Figure 4.5 shows two geometries: two PIFAs are located orthogonally or parallel.

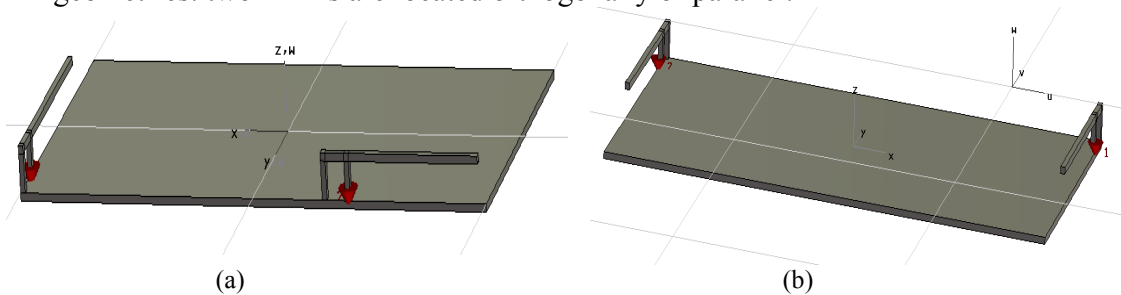


Figure 4.5. geometry of two PIFA antennas: (a) two PIFAs located orthogonally. (b) two PIFAs located parallel.

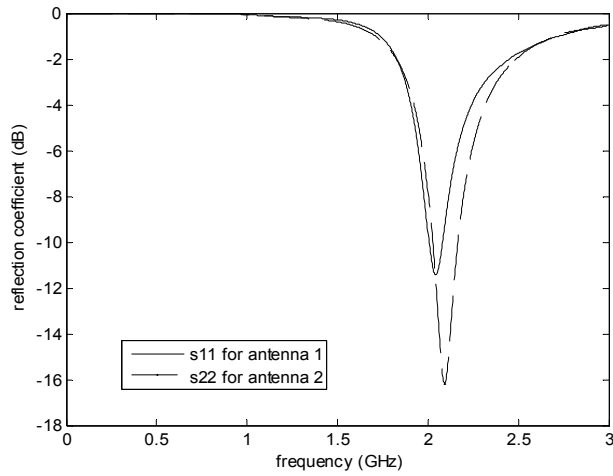


Figure 4.6 comparison of reflection coefficient between two antennas in Figure 4.5(a).

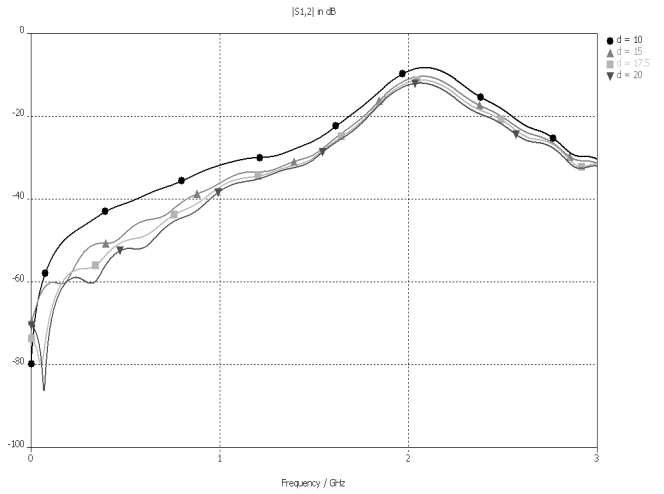


Figure 4.7. different performance of S12 against different distance of the two PIFA antennas in Figure 4.5(a).

Figure 4.5 shows two geometries of two PIFA antennas. And figure 4.6 illustrates the different performance of reflection coefficient in this case of Figure 4.5(a). We can see that two PIFA antennas have different reflection coefficients. These two antennas are not uncorrelated, and they effect on each other. From the Figure 4.7, we can obtain that the coupling between two PIFAs becomes weaker when the distance between the two PIFAs becomes larger.

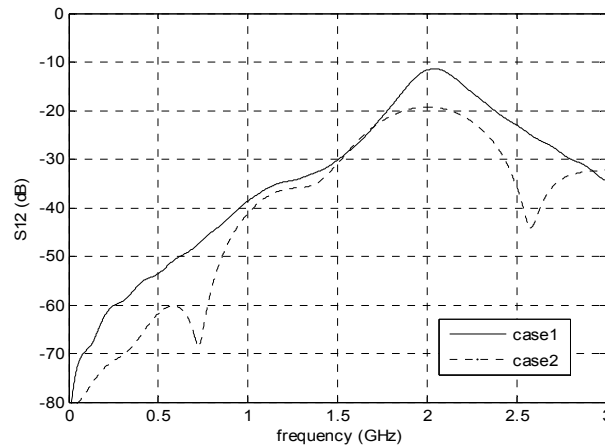


Figure 4.8. comparison of S12 between two cases: case1 for Figure 4.5(a), case 2 for Figure 4.5(b).

As shown in Figure 4.8, when one antenna is located at the top and the other one is located at the bottom, shown as Figure 4.5(b), the coupling between these two antennas will decrease around 8 dB, compared with the case when the two antennas are located orthogonally, as Figure 4.5(a).

### 4.3 Correlation Coefficient

To study the correlation coefficient of two PIFA antennas on PCB, Several geometry cases were considered and built in the simulation. Since the battery, the camera, the speaker, and other components occupy space of the central part in a real mobile phone, it

is advisable to mount the antennas at the edge of the PCB. Figure 4.9 and Figure 4.10 show four main geometry cases which was focused on. The geometries in Figure 4.9 are referred to orthogonal case in this work, and that in Figure 4.10 are called parallel case.

The designed ground plane has the dimension  $100 \times 50 \text{ mm}^2$ , which is the same as the standard stick type phone models. The dimensions of designed antennas has the length 33.5 mm, height 5.8 mm, and the space between the ground point and feed point is 5 mm. The antenna wire radius is 1 mm. For the orthogonal case, one antenna is mounted on the top of the ground plane, and the second antenna is placed either on the left, shown in Figure 4.9(a) or the right edge, shown in Figure 4.9(b). The distance between the antennas is changed by moving the second antenna along the line as shown in Figure 4.9. As the distance is changed, the correlation coefficient will change as well. We will focus on the relation between correlation coefficient and the distance between two PIFA antennas. For the parallel case, as shown in Figure 4.10, one antenna is mounted on the top of the plane, and the second antenna is placed on the bottom, but the radiation direction is either the same or opposite.

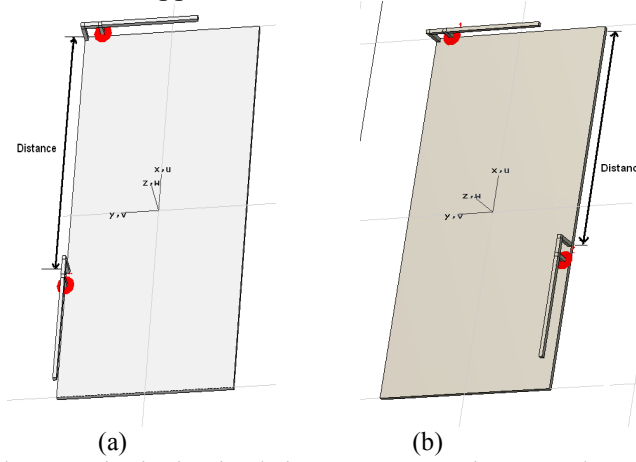


Figure 4.9 Orthogonal geometries in the simulation. One antenna is mounted on the top of the plane, and the second antenna is placed on the left (a) or on the right (b).

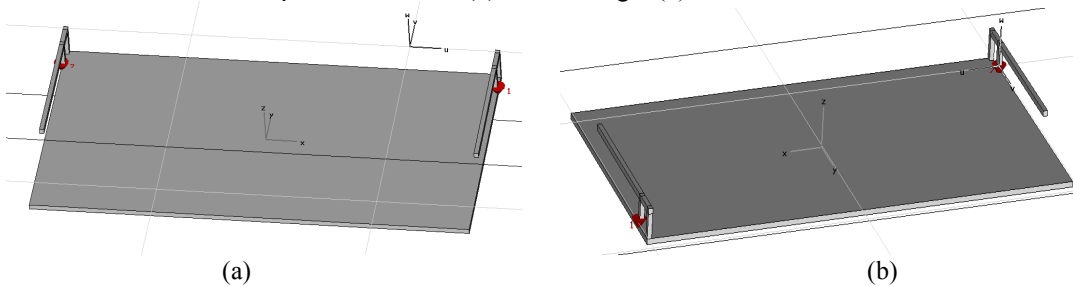


Figure 4.10 Parallel geometries in the simulation. One antenna is mounted on the top of the plane, and the second antenna is placed on the bottom, but the radiation direction is either the same (a) or opposite (b).

For the simulated geometries shown in Figure 4.9, correlation coefficient of two PIFA antennas both calculated from far-field function and S parameters is shown in Figure 4.11. It has a minimum correlation coefficient when the second antenna is located at the left side edge and at far bottom end of the PCB. In this case, the correlation coefficient will decrease as the distance between two antennas increases. However for the case

where the second antenna is located at the right side edge, the correlation coefficient does not change significantly as the distance is increased. It is also interesting to note that the performance differs a lot when we put the other antenna on the left side or on the right side. When two antennas are located nearer than 20mm, the right side is a better choice, but the left side becomes the better choice when the distance gets larger.

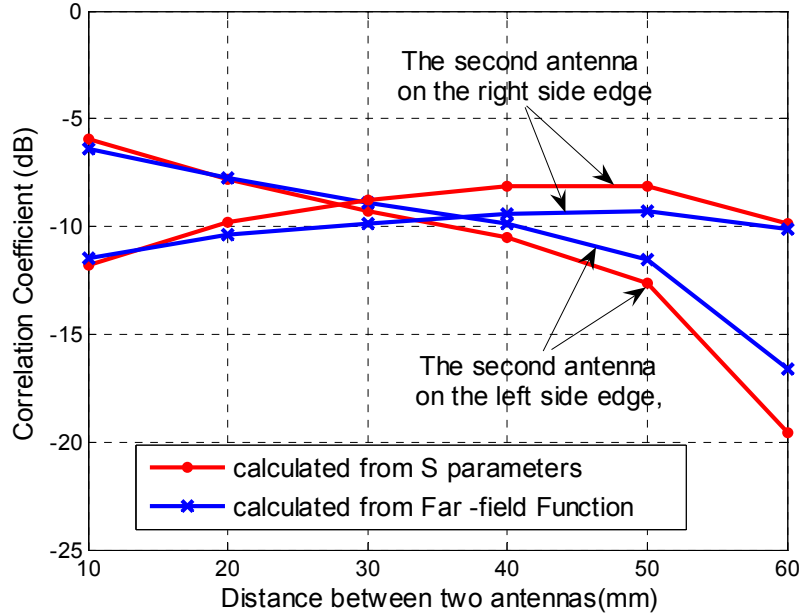


Figure 4.11. The correlation coefficient against distance between two PIFAs calculated both from Far-field and S parameters.

#### 4.4 Diversity Gain

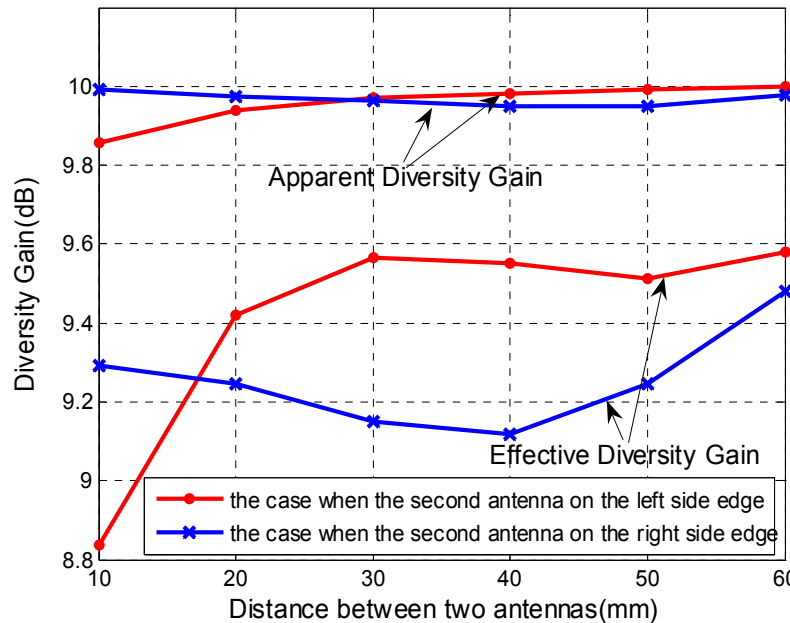


Figure 4.12. The diversity gain against distance between two PIFAs

calculated from Far-field.

Figure 4.12 shows the comparison of apparent diversity gain and effective diversity gain in both cases from far-field function. The maximum effective diversity gain is obtained as 9.58 dB in the simulation when the second antenna is located at the left side edge and at far bottom end of the PCB.

For the parallel cases shown in the Figure 4.10, the correlation coefficient and apparent diversity gain are calculated and listed below in table 4.1. Low correlation and high diversity gain are obtained in both cases, indicating that these two antennas are nearly uncorrelated.

Correlation Coefficient/DG(dB)	Figure 4.10(a)	Figure 4.10 (b)
From far-field	0.04/9.996	0.05/9.994
From S parameter	0.017/9.999	0.011/9.999

table 4.1 Correlation coefficient and diversity gain for the geometries in Figure 4.10.

## 4.5 Measurement

To testify and confirm the results in simulation, prototypes are manufactured and measured. The practical measurements of the prototypes were conducted for calculating the correlation coefficient and consequently the diversity gain. In simulations, the correlation coefficient is calculated both from S parameters and Far-field function. In measurements, S parameters is measured using Network Analyzer and Far-field pattern measurements are performed in a scattered field chamber(SFC).

### 4.5.1 Scattered field chamber(SFC)

The Scattered field chamber, which also known as mode-stirred chamber, is a rectangular metal box or enclosure which contains and supports many resonant cavity modes simultaneously. The chamber has been used for electromagnetic compatibility measurement. Mostly it has been used for electromagnetic immunity testing, where it is desirable to put the test object under radiation from all directions. But it is also possible to measure the radiation efficiency, the total radiated power by mobile phones, impedance of terminal antennas, diversity gain and receiver sensitivity in the chamber.

The idea and functionality of a reverberation chamber it to insert power by an antenna inside the closed chamber and then stir the cavity mode structure with a mechanical stirrer or tuner. The movement of the stirrer then changes the boundary for the mode structure and provides an electromagnetic field environment that is statistically described. The average of all the collected power samples created by moving the stirrers is then a statistical estimate of the mean received power with some statistical confidence. Controlling the stirrers can repeat the propagation environment inside the chamber [8].

The chamber has many resonant excited modes, which are stirred by moveable objects inside the cavity. Therefore, different, independent field distributions are generated. Together all, the independent field distributions will represent a statistically isotropic



field, i.e., the test object will receive signals from all directions in space with multi-path environment.

in the measurement, one antenna is measured at a time while the other one is terminated with a 50 Ohm load. In every measurement in the SFC, a large number of the data samples are collected to make the result accurate. The number of samples chosen was 10,000.

#### 4.5.2 Error Tolerant Analysis

When the prototype is manufactured, it is difficult to ensure the dimension of the manufactured PIFA antenna is the same as that of design. Hence it is necessary to do the error tolerant analysis before measurements. Error Tolerant Analysis(ETA) here means changing the dimension of the PIFA antenna slightly in the simulation to see whether the bandwidth, resonant frequency, correlation coefficient still are acceptable to meet the design requirements. Table 4.2 lists different performance when the length of the PIFA antenna was slightly changed.

Length(mm)	Resonant Frequency(GHz)	Bandwidth(GHz)	Correlation Coefficient	Diversity Gain(dB)
30	2.3174	2.12 - 2.1517	0.13	9.96
31.5	2.2107	2.0365 - 2.4017	0.06	9.99
<b>32.5</b>	<b>2.091</b>	<b>1.94 - 2.27</b>	<b>0.04</b>	<b>9.99</b>
33	2.0251	1.8962 - 2.1977	0.03	9.99
33.5	2.0036	2.12 - 2.1517	0.03	9.99

Table 4.2 Parameters evaluation of PIFA antenna in simulation when the length of the antenna is changed.

From table 4.2, it is easily seen that the bandwidth, the correlation coefficient and diversity gain do not change significantly when the length is changed slightly, for instance, 1mm both increase and decrease. Thus 1 mm's distortion in the measurement can be tolerated.

### 4.5.2 Measurement using Network Analyzer

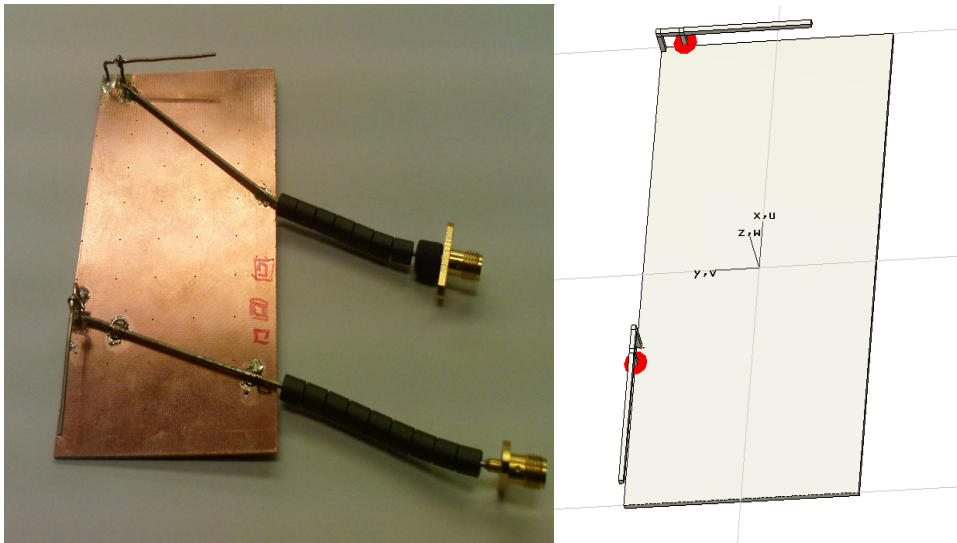
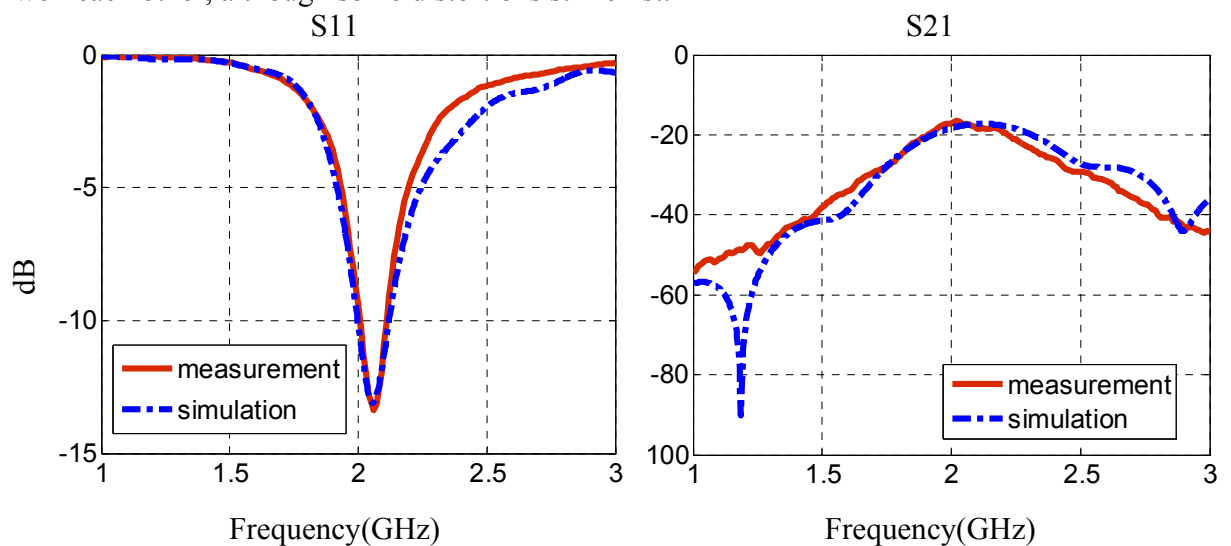


Figure 4.13 Prototype in the measurement and geometry in the simulation, one antenna is located at the top of PCB, and the other one is located at left side edge, two antennas are separated by 60mm.

Figure 4.13 shows the prototype in the measurement and the geometry in the simulation. In this measurement, one antenna is located at the top of PCB, and the other one is located at left side edge, two antennas are separated by 60mm.

Firstly, S parameters was measurement using Network Analyzer. Figure 4.14 shows the comparison of simulated S parameters and measured results for prototype shown in Figure 4.13. The simulated and measured S11 on Smith Chart are plotted together in Figure 4.14. From Figure 4.13, 4.14, the simulated and measured S parameters match well each other, although some distortions still exist.



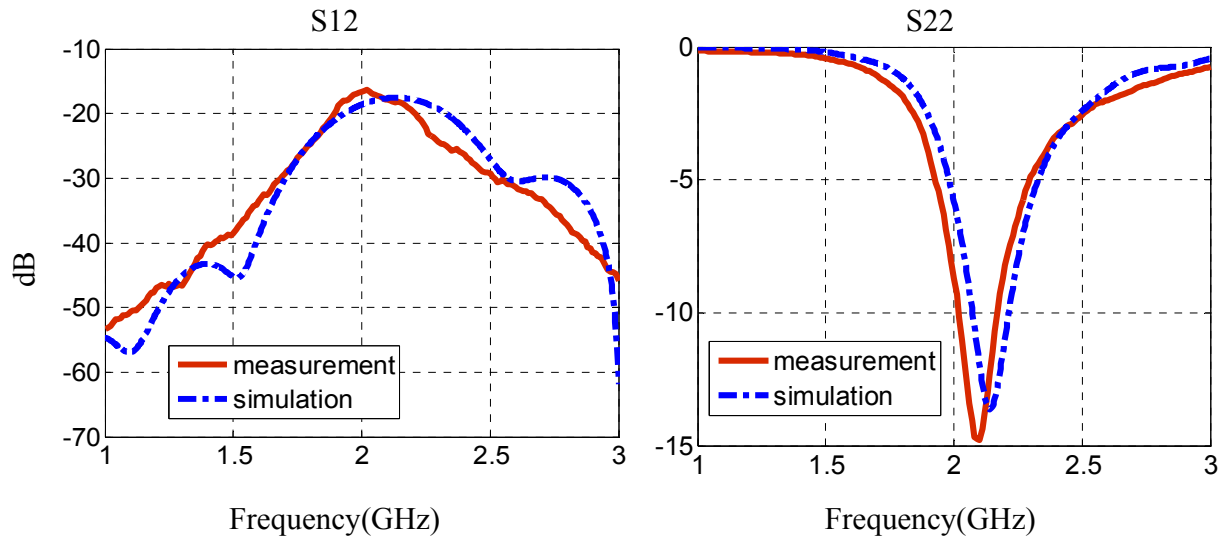


Figure 4.14 Comparison of S parameters between simulation and measurement from Network Analyzer.

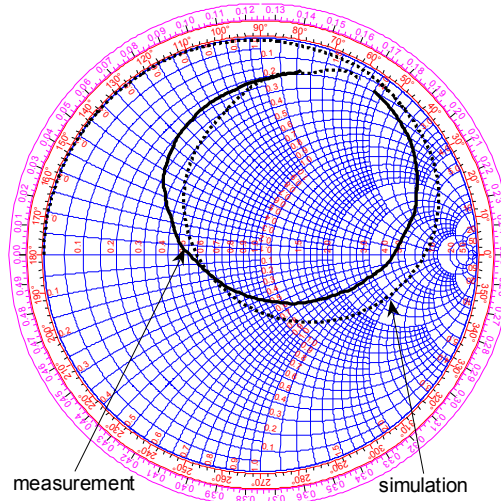


Figure 4.15 Comparison of simulated and measured S11 on Smith Chart

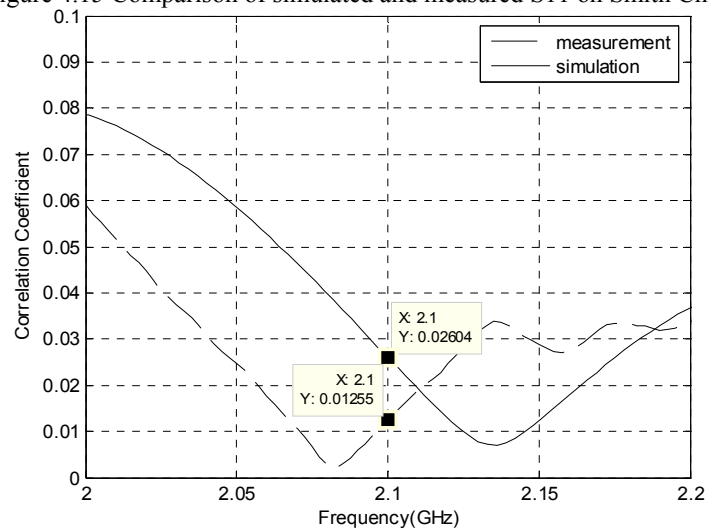


Figure 4.16 Correlation coefficient calculated from simulation and measurement at 2.1 GHz

Figure 4.16 shows the correlation coefficient calculated from simulated and measured S parameters, respectively. It is easily obtained that the correlation coefficient has the same trend against frequency in simulation and measurement. At 2.1 GHz, the correlation coefficient is very low both in simulation and measurement, consequently similar apparent diversity gain can be obtained from the calculated correlation coefficient. The results are listed in table 4.2. However the embedded element efficiency can not be measured using Network Analyzer, we have no idea about how the effective diversity gain change in simulation and measurement. Therefore Scattered field chamber will be used in next step to measure the diversity performance of that prototype.

2.1GHz	Simulation	Measurement
<b>Correlation Coefficient</b>	<b>0.026</b>	<b>0.013</b>
<b>Apparent Diversity Gain(dB)</b>	<b>9.996</b>	<b>9.998</b>

Table 4.2 Comparison of simulated and measured correlation and apparent diversity gain.

### 4.5.3 Measurement in Scattered field chamber

In the measurement in Scattered field chamber, one antenna is measurement at a time while the other one is terminated by 50 Ohm load. When both antennas are measurement, a set of signal power data for each antenna is collected. After calculating the cumulative probability against the relative signal power in Matlab, the diversity gain can be easily read directly from Figure 4.17 which shows the cumulative probability against relative signal power. The relative signal power used here is the instantaneous signal power related to the mean signal power of one antenna, since the values of mean signal power from both antennas are almost the same in this measurement. The selective combining scheme is utilized, always the stronger signal is selected. Figure 4.17 shows the selective combining scheme in the measurement during a period of time.

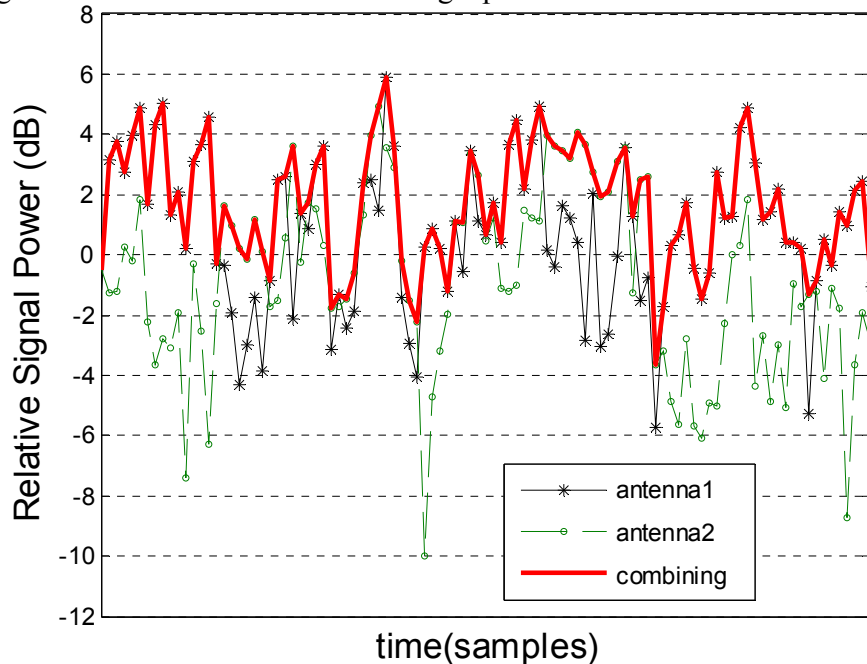


Figure 4.17 Antenna combining using selective combining scheme

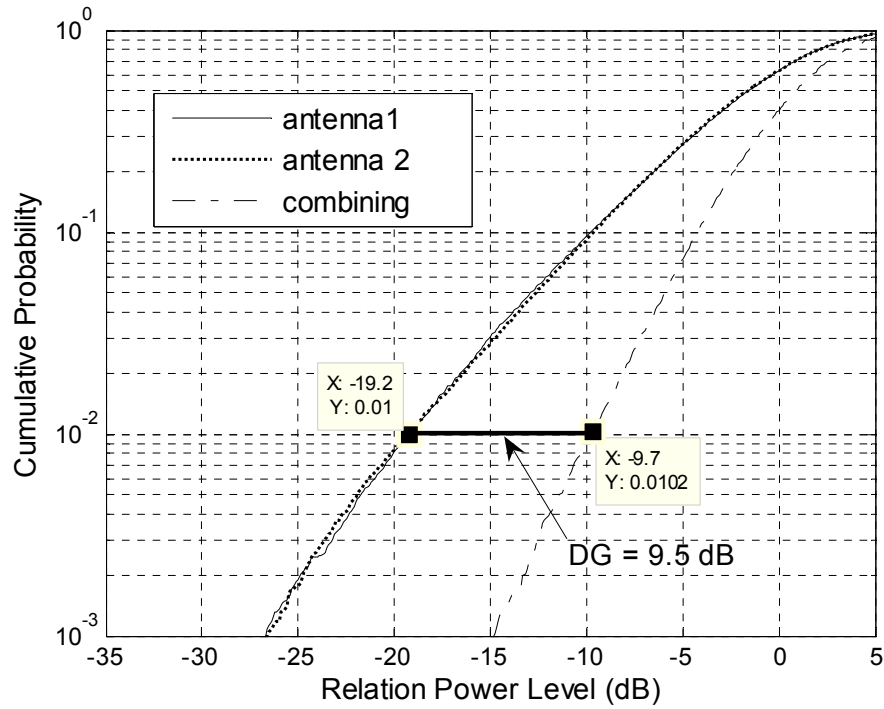


Figure 4.18 Diversity gain obtained from Scattered field chamber for the prototype shown in Figure 4.13.

Figure 4.18 shows the apparent diversity gain measured in the scattered field chamber for the prototype shown in Figure 4.10. 9.5 dB apparent diversity gain is obtained in this measurement. When the embedded element efficiency is taken into account, 7.74 dB effective diversity gain is obtained.

## 5. Effect of Matching Networks on Diversity Performance and Optimized in MPA

### 5.1 Matching Networks

The need for matching networks arises in order to deliver maximum power to a load or to perform in a certain desired way. The matching networks are lossless in order not to dissipate any of the signal power. In this chapter, we are concerned with the effect of matching networks on diversity performance. Lumped elements are used for the matching purpose. Lumped-parameter elements such as conventional inductors and capacitors have been introduced into prominence for impedance-matching purpose, since they are not only simple to design but quite practical. The basic lumped-element impedance-matching circuit is a circuit consisting of a parallel-connected or series-connected reactive element. Generally, four main types of lumped-element are derived as: series L, shunt L, series C, and shunt C. L here means inductor and C presents capacitor [13] and [14].

### 5.2 Introduction of MPA

MPA (Multi Port Antenna evaluator) is developed by SP Technical Research Institute of Sweden for the purpose of developing methods so that new antenna solutions and system technologies for mobile terminals efficiently can be evaluated and optimized in the future wireless communication system.

MPA uses data from full wave electromagnetic simulations in combination with circuit simulations for calculation of a number of antenna parameters, such as total radiated power, efficiency, radiation pattern, near field, correlation, apparent diversity gain, and etc. MPA is combined with a global optimization scheme, so it can be used to optimize for efficiency, correlation and so on [15].

Figure 5.1 shows the start up view in MPA. The full wave electromagnetic simulator used in this work is CST MWS, the circuit simulator used is CircSim, which is an auxiliary program with MPA.

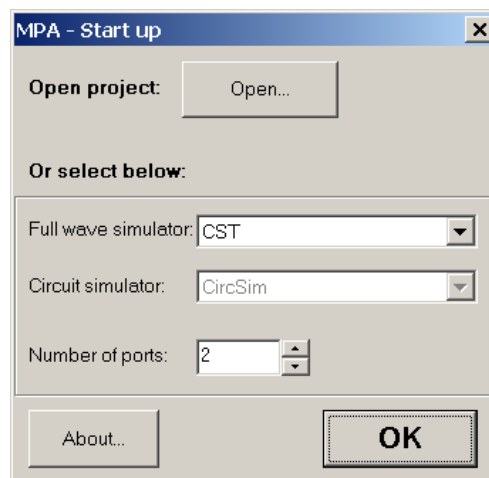


Figure 5.1 Start up in MPA

The embedded element patterns used in Figure 5.2 are from simulated far-field patterns in MWS. Z-matrix here is transferred from the simulated S matrix at a fixed frequency point. The circuit selected is shown in Figure 5.3 which is the interface of Circuit Simulator. The file which defines Z1 component in Figure 5.3 has to be the same as Z-matrix setting in Figure 5.2. After loading the files, the functions for calculations are available. In this work, we are concerned with efficiency and correlation, thus we have to define them before calculation. The interfaces for definition are shown in Figure 5.3.

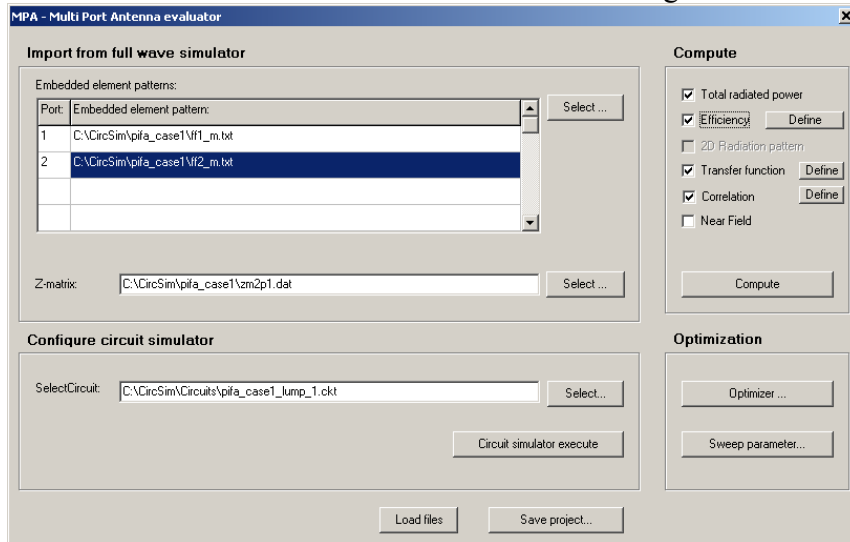


Figure 5.2 File import view in MPA.

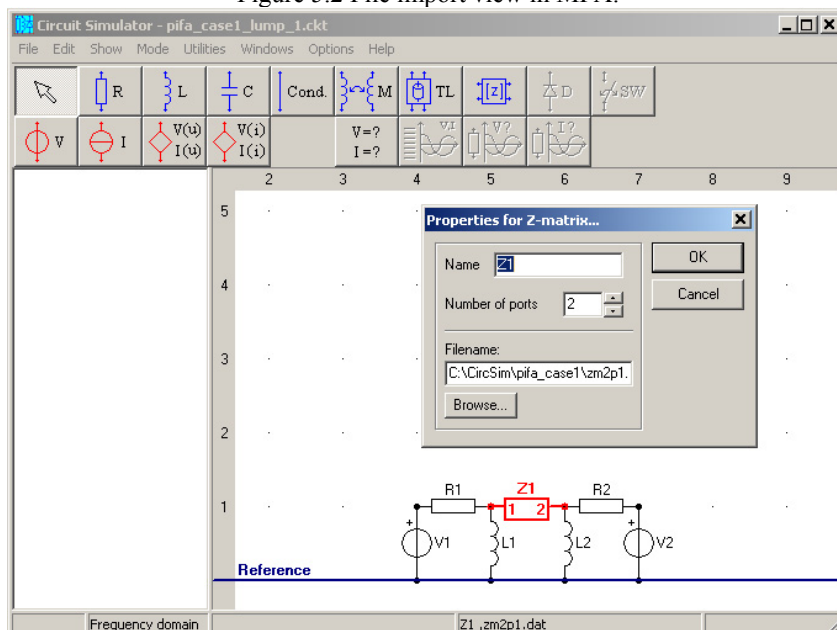


Figure 5.3 Interface in Circuit Simulator.

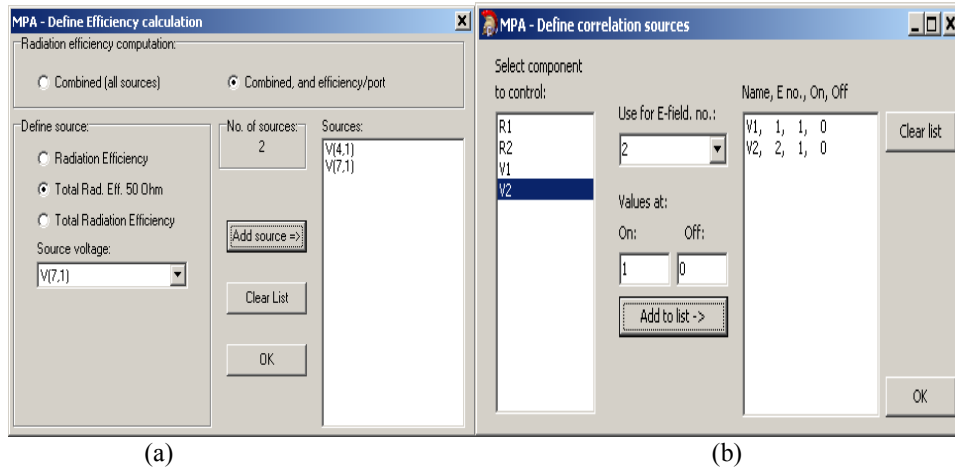


Figure 5.4 Definition interface for efficiency (a) and correlation (b) in MPA.

In efficiency definition, the number of source voltage can be read from the circuit simulator, total radiation efficiency 50 Ohm is selected since when one port is calculated assuming the other one is terminated by a 50 Ohm load. In correlation definition, V1, V2 are chosen for the calculating the correlation of radiation patterns.

Furthermore, optimizer, shown in Figure 5.5, can be used after the normal calculations. In this work, two shunt inductors are used as matching circuit, as in Figure 5.3. Target frequency has to be defined first, then the maximum and minimum values of both inductors are set. The target here is both high efficiency and low correlation.

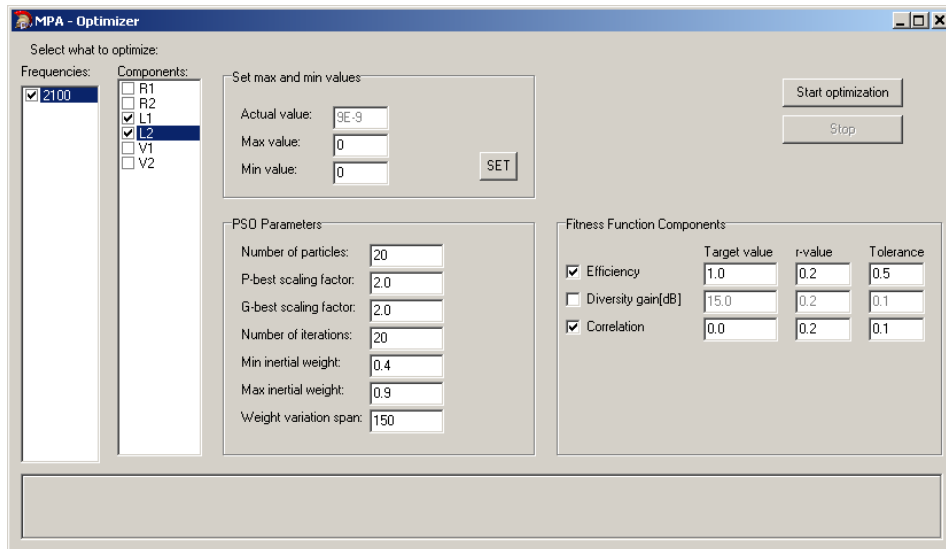


Figure 5.5 Optimization interface in MPA.



### 5.3 Simulation and Measurement Without Matching Network

A second prototype was manufactured to study the effect of matching networks on diversity performance. The dimension of the prototype is defined as in Figure 5.6.

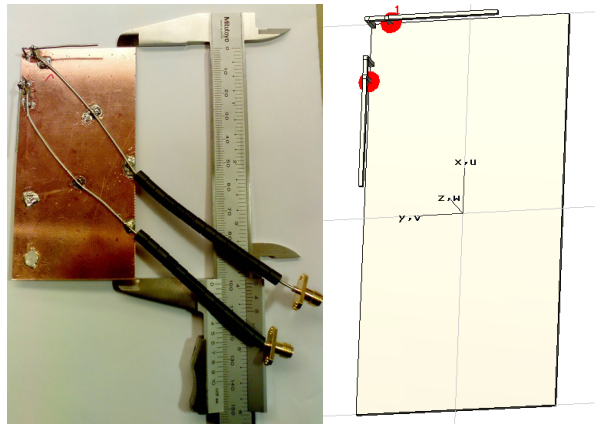
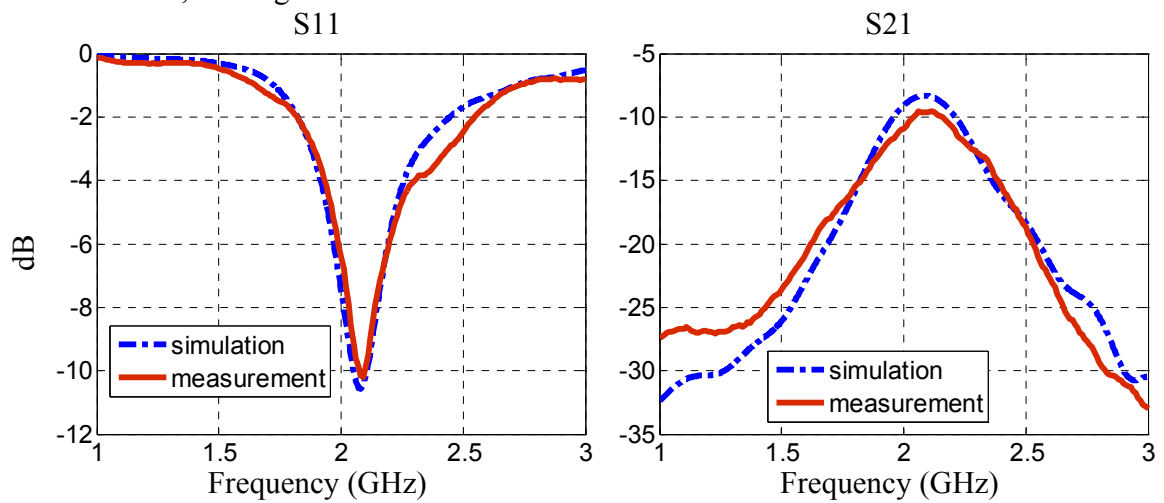


Figure 5.6 Prototype in the measurement and geometry in the simulation, one antenna is located at the top of PCB, and the other one is located at left side edge, two antennas are separated by 10mm.

In the Figure 5.7, the simulated and measured S parameters are compared, they match well each other, although some distortions still exist.



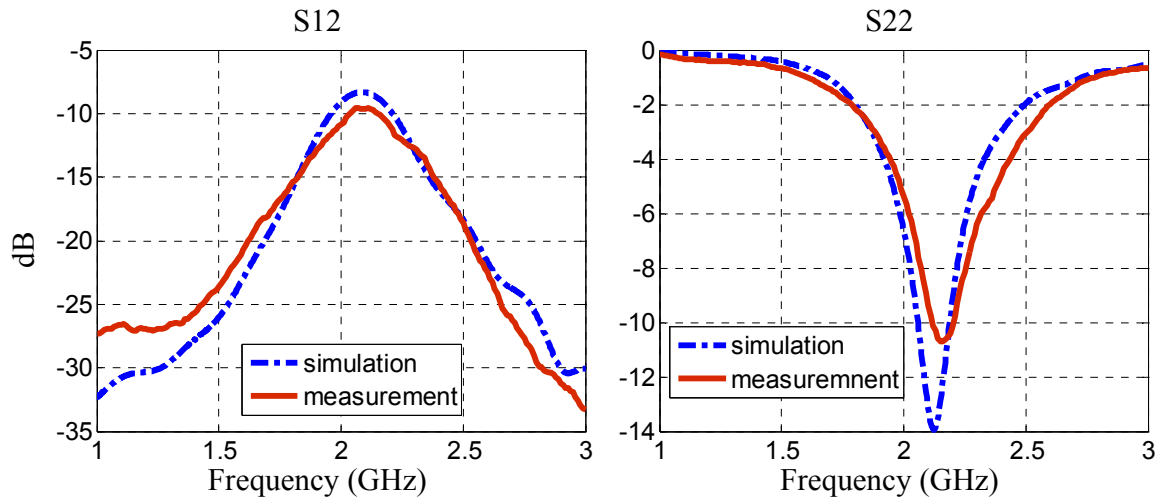


Figure 5.7 Comparison of simulated and measured S parameters without matching networks from Network Analyzer.

#### 5.4 Simulation and Measurement With Matching Network and Optimization

In the simulation, two shunt inductors are used as the matching network, as in Figure 5.8 (a). The required values of the matching elements are easily found using the Smith Chart. The approximate value for each inductor is initially defined as 5 nH. In Figure 5.8 (b) and 5.8 (c), the lumped element is connected with the feeding point and ground for each antenna.

After the simulation, we found that 5nH is not the accurate value for perfect matching. Then MPA was used in order to optimization the values of two inductors, as shown in Chapter 5.2. The target is not only low correlation coefficient, but also relative high embedded element efficiency, since effective diversity gain, in which the efficiency is taken into account, is more important in diversity antenna system. The value for inductor 1 becomes 4.56 nH and the value for inductor 2 becomes 9 nH after the optimization.

Using these two optimized inductors to do the simulation again, better S parameters performance are obtained, shown in Figure 5.9 and 5.10. All the simulated and calculated parameters both from CST MWS and MPA are listed in Table 5.1 to compare the diversity performance between with and without matching networks and to show how benefit we can obtain from matching networks for diversity performance.

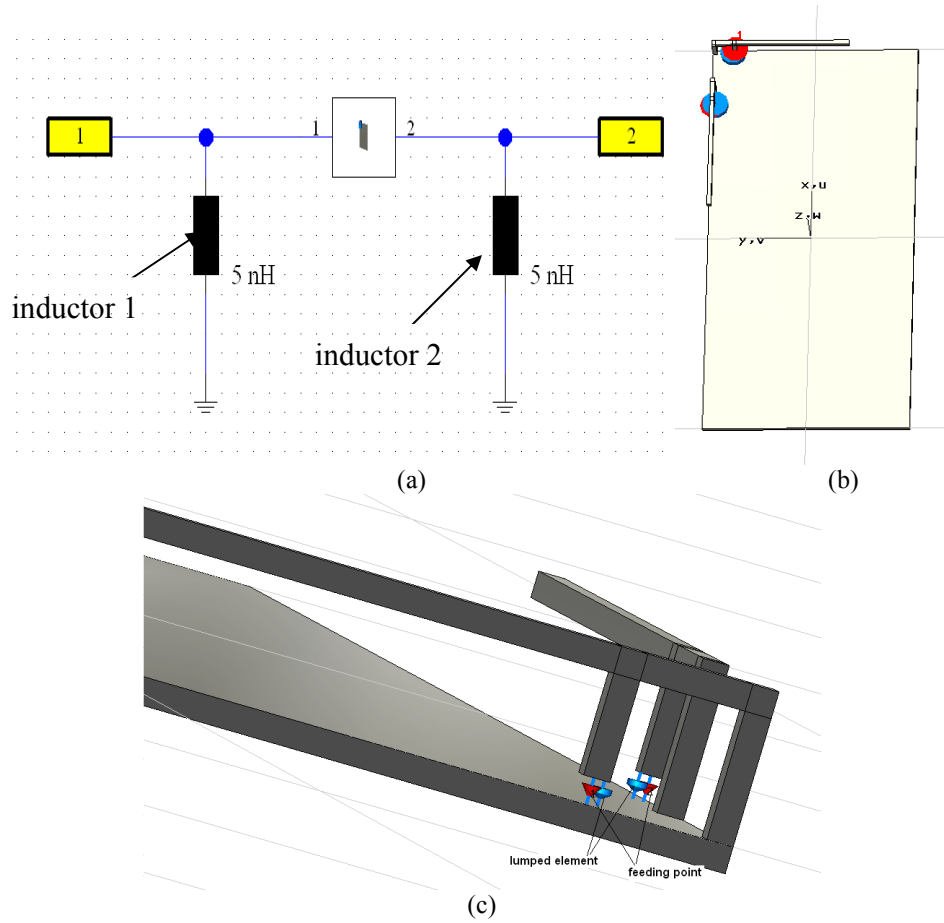
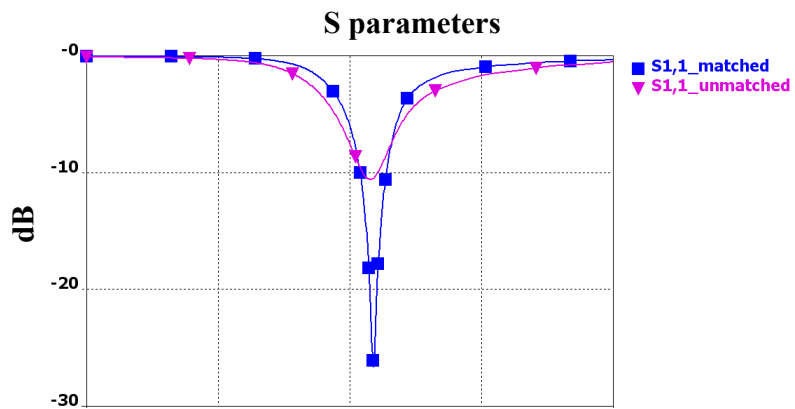


Figure 5.8 Matching networks in simulation. (a) two shunt inductors as matching network connected to the two ports diversity antenna system. (b) geometry of two PIFA antennas with lumped elements. (c) lumped elements are shunt connected.



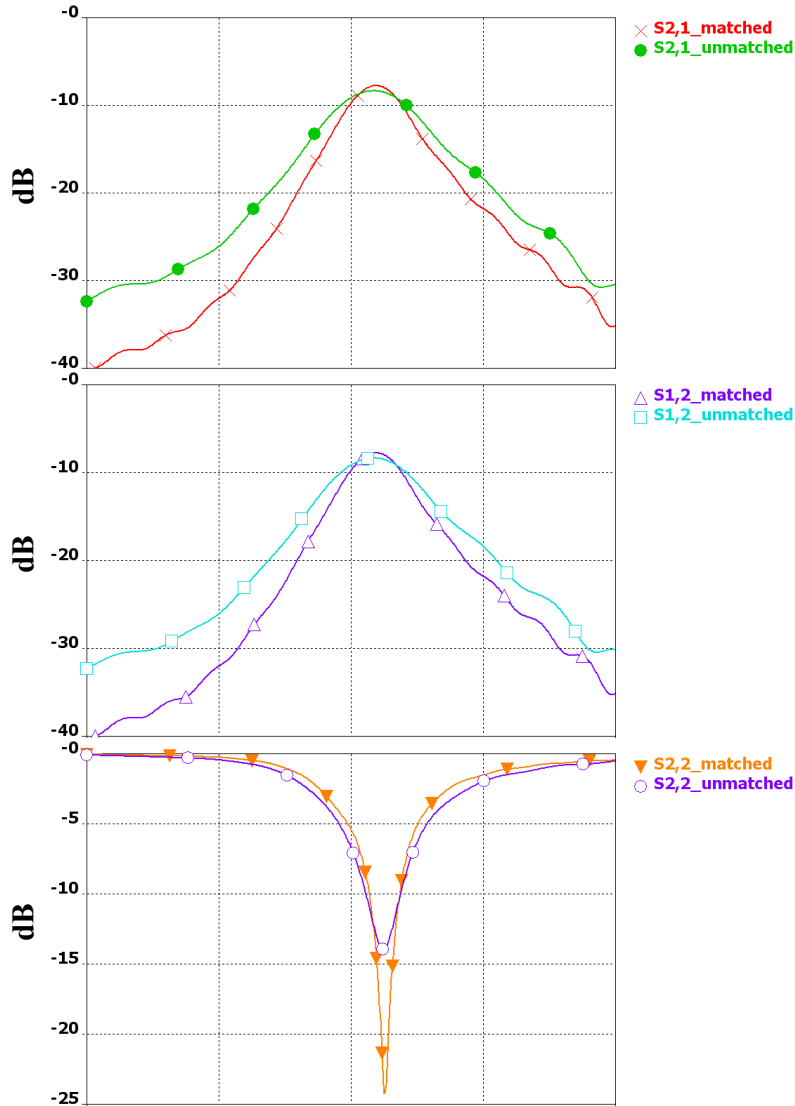


Figure 5.9 Simulated S parameters with and without matching networks

Figure 5.9 shows the comparison of simulated S parameters between before and after using matching networks. With the effect of matching networks, the return loss, both S<sub>11</sub> and S<sub>22</sub>, is reduced from -10dB to around -25dB at 2.1 GHz, which is the desired resonant frequency. From the plot of S<sub>12</sub> and S<sub>21</sub>, the coupling between these two antennas at resonant frequency increases a little bit, although not obviously. However the increase of coupling is a potential factor which effects the diversity performance, since the embedded element efficiency will probably be reduced due to the increase of coupling. Figure 5.10 shows S<sub>11</sub> and S<sub>22</sub> on Smith Chart, it is very close to the original point on Smith Chart at the resonant frequency in both of S<sub>11</sub> and S<sub>22</sub>, which means the matching is achieved after optimization.

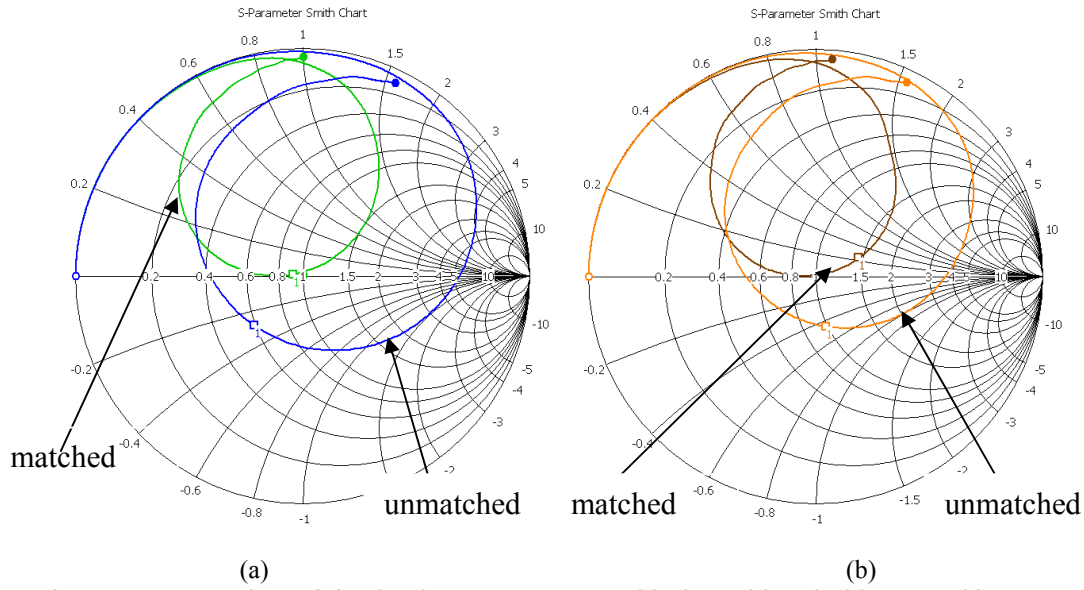


Figure 5.10 Comparison of simulated S parameters on smith chart with and without matching networks. (a) S11. (b) S22.

		<b>Embedded Elements Efficiency</b>	<b>Correlation Coefficient</b>	<b>Apparent DG (dB)</b>	<b>Effective DG(dB)</b>
CST	<b>without</b>	<b>0.7451</b>	<b>0.25</b>	<b>9.86</b>	<b>8.84</b>
		<b>0.7907</b>			
	<b>with</b>	<b>0.8147</b>	<b>0.11</b>	<b>9.97</b>	<b>9.08</b>
		<b>0.7846</b>			
	<b>optimized</b>	<b>0.8112</b>	<b>0.09</b>	<b>9.98</b>	<b>9.07</b>
		<b>0.789</b>			
MPA	<b>without</b>	<b>0.70958</b>	<b>0.25</b>	<b>9.86</b>	<b>8.64</b>
		<b>0.75648</b>			
	<b>with</b>	<b>0.6933</b>	<b>0.12</b>	<b>9.97</b>	<b>8.38</b>
		<b>0.6304</b>			
	<b>optimized</b>	<b>0.67358</b>	<b>0.1</b>	<b>9.98</b>	<b>8.26</b>
		<b>0.67358</b>			

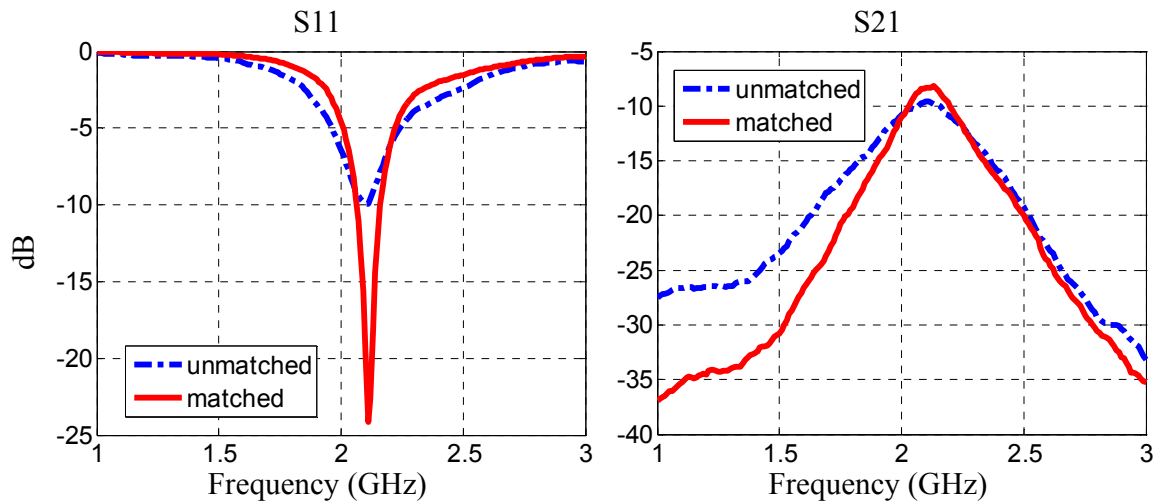
Table 5.1 Simulated diversity performance both from CST and MPA

The parameters simulated and calculated both from CST and MPA are listed in Table 5.1. Comparisons between CST and MPA have been done to verify the results. On the other hand, comparisons among without, with matching networks and with optimized matching networks have been done as well to illustrate whether the matching networks can improve the diversity performance in this simple case that two PIFA antennas are mounted on PCB and what benefit can be obtained from matching networks. The embedded element efficiency shown in the table presents the efficiency from each antenna, the stronger efficiency is used when calculating the effective diversity gain.

From the results, it is easily obtained that the correlation coefficient is reduced from 0.25 to 0.1 after adding matching networks and optimizing. Consequently, 0.12dB additional apparent diversity gain is obtained. However, the effective diversity gain obtained from the calculation in CST is quite different from that in MPA due to the different calculated efficiency.<sup>3</sup> In the calculation in CST, 0.23dB additional effective diversity gain is obtained. On the contrary, the effective diversity gain is reduced by 0.38dB in calculation in MPA. Furthermore, it is interesting to point out that the effective diversity gain decreases rather than increases after optimization, compared with that of non-optimized, although the correlation coefficient is reduced. It is due to the increased coupling and reduced efficiency. It makes sense that it is very important to find the trade-off between correlation coefficient and embedded element efficiency when designing a diversity antenna system with matching networks.

In measurement, the prototype shown in Figure 5.6 is used to compare the results of without and with matching networks. In simulation, the optimized inductor values are 4.56 nH and 9 nH, respectively. However, there is no inductors of these values in the laboratory, 4.7nH and 10nH inductors are used instead in the measurement. The inductors are too tiny to show here.

Figure 5.11 shows the measured S parameters without and with matching networks. They agree well with simulated results shown in Figure 5.9. Figure 5.12 shows the measured return loss on Smith Chart, which agree well with simulated results shown in Figure 5.10 as well. Matching is achieved in the measurement.



<sup>3</sup> Different methods are used in CST and MPA for the calculation of efficiency. The reason why the obvious difference exists has been checking.

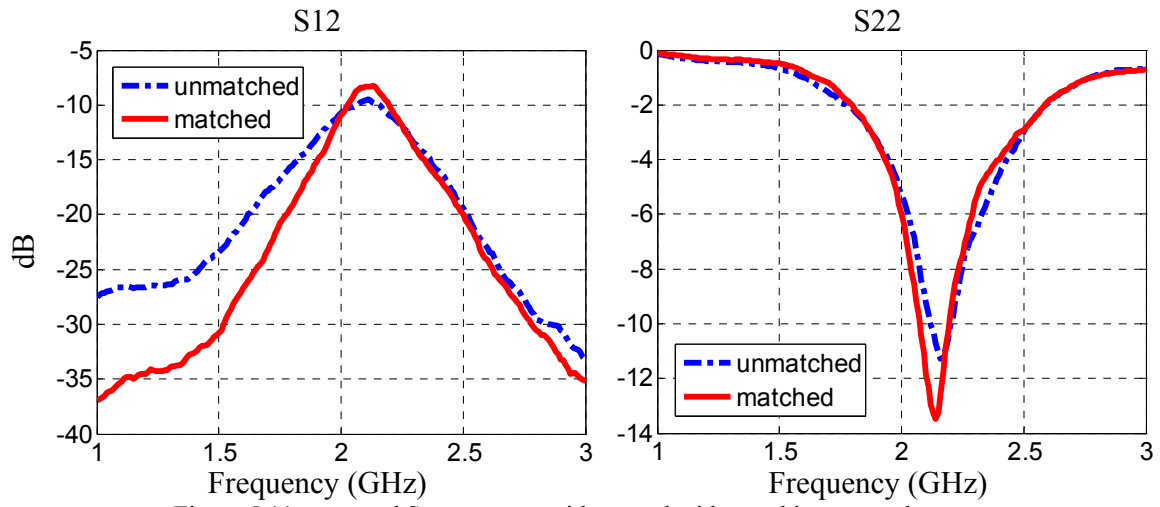


Figure 5.11 measured S parameters without and with matching networks

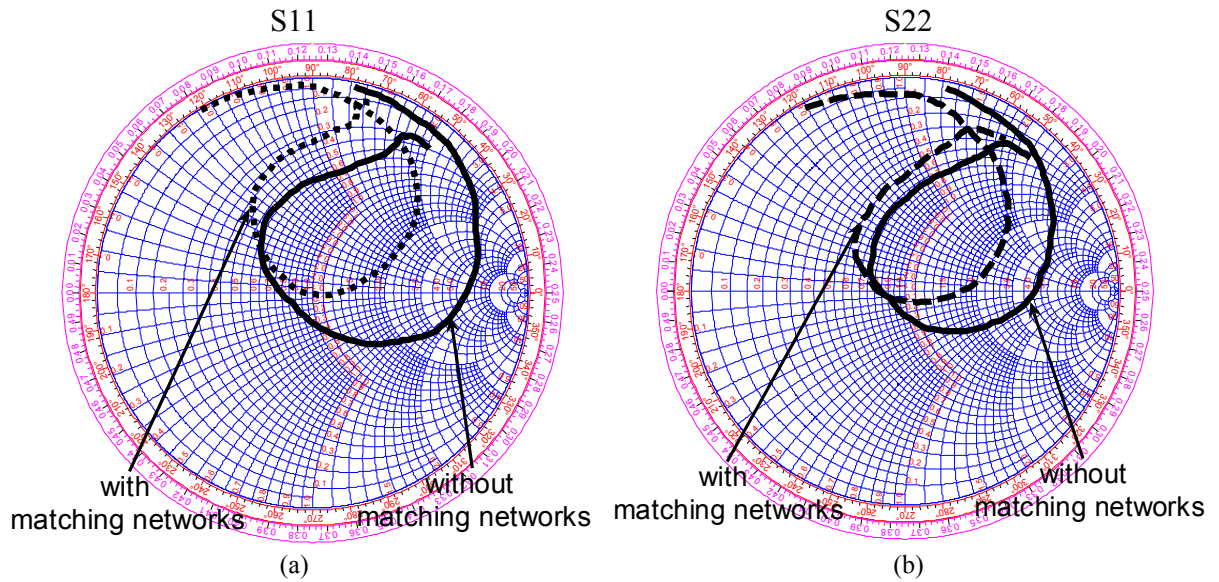
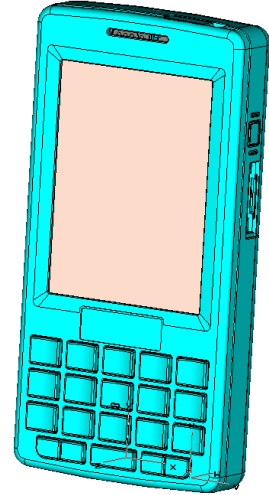


Figure 5.12 Comparison of measured S parameters on smith chart with and without matching networks. (a) S11. (b) S22.

## 6. Study of Diversity Performance in Full Phone Case

In this chapter, study of diversity performance has been done by adding an extra antenna for UMTS 1 Band inside an existing mobile phone, Sony Ericsson M600, shown on the right. While adding an extra antenna inside an existing mobile terminal, there mainly are two aspects to be considered. One is the sufficient space to put an extra antenna. Inside a mobile terminal, many components are equipped advisably with compact, occupying a significant proportion of the space. Thus the edge of the terminal is considered to be the possible placement. The second aspect is the influence on the performance of the antenna from other components inside the mobile terminal. A number of components exist inside the mobile phone, such as loudspeakers, cameras, vibrators and batteries, which are more important to design the antenna and antenna position, since they are always placed near from antennas. In the simulations, we found that the battery has the most important effect when evaluating the diversity performance of the system. There also exist some plastic components which have the effect on the resonant frequency.



For the purpose of convenience, the original antenna which is used in the existing mobile phone is called main antenna; the adding one is called diversity antenna. Many factors have to be evaluated to ensure the diversity antenna system has a good performance. First of all, both main antenna and diversity antenna have to have low return loss at the resonant frequency. Secondly, the coupling between main antenna and diversity antenna must be low. Furthermore, the diversity antenna can not have more than one resonant frequency, which is likely to occur when the diversity antenna is equipped very close to the battery. Finally and most important, the correlation coefficient between main antenna and diversity antenna must be ensured to be very low and the efficiency of both antennas do not reduced, then better diversity gain is obtained.

PIFA antenna, which has been presented in chapter 3, is chosen in this part. However the dimension of the PIFA used in chapter 3 has been modified to match another resonant frequency due to the effect from the plastic components. In the simulation, a number of tests, with different diversity antenna placements, have been done. In the following part, some of tests including geometries and S parameters are presented to show the different performance of available and unavailable placements.

### 6.1 Dimension selection

As discussed in previous part, the plastic components have the effect on the resonant frequency. The dimension of the PIFA antenna designed in chapter 3 have to be changed to meet the resonant frequency and bandwidth requirements. Finally, the length ( $L$ ) of the PIFA antenna is chosen as 21 mm and the distance ( $dv$ ) between feed point and ground



point is chosen as 3 mm for the purpose of easily matching. The return loss of both main antenna and diversity antenna is shown in Figure 6.1.

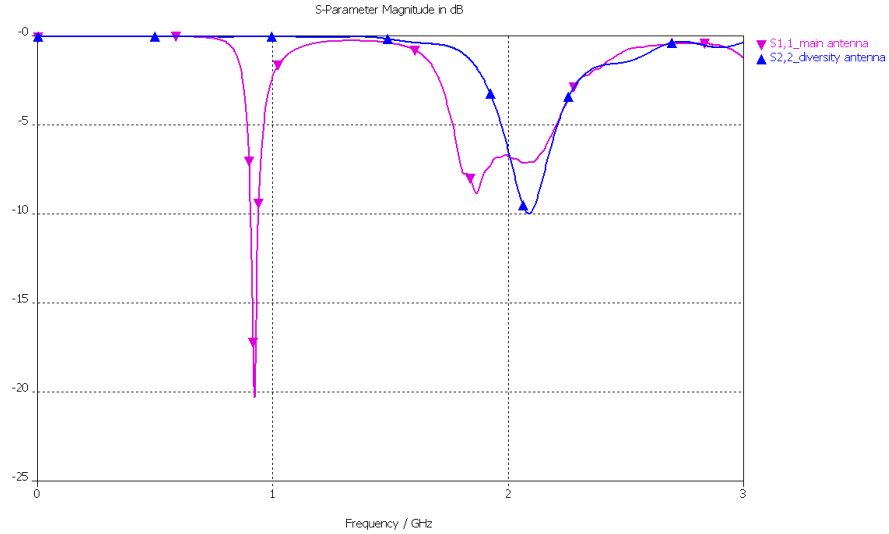


Figure 6.1 Return loss of both main antenna and diversity antenna.

## 6.2 Unavailable Cases of Placements

### Case 1.

The battery is grounded on the PCB but not fully, which means there exist some plastic component between the battery and PCB, shown in Figure 6.1.

The S22 in this case are plotted together and compared with the desired one in Figure 6.2. In this placement, the diversity antenna has very bad performance. The return loss is quite high and do not cover the requirement the frequency bandwidth. Another resonant frequency appears due to the battery's effect, since the battery acts as another resonant source.

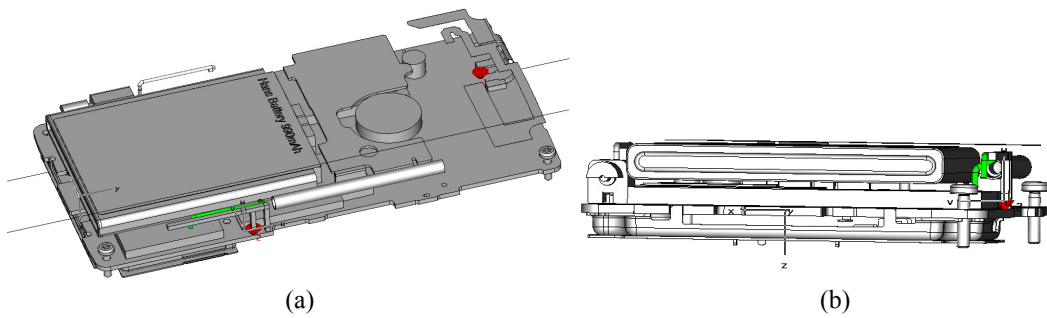


Figure 6.1 Geometry of case 1. (a) view from the top. (b) view from the bottom.

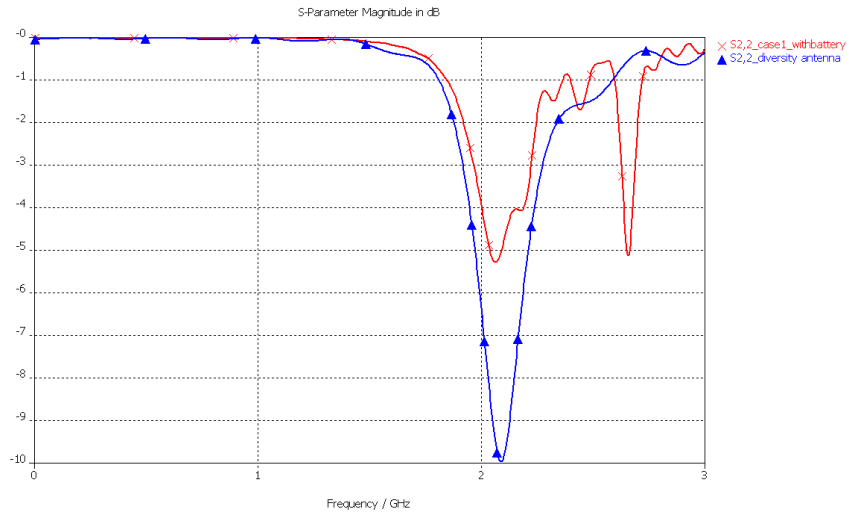


Figure 6.2 Comparison of S22 between case 1 and the desired case.

## Case 2.

The battery is fully grounded on the PCB, which means that there is no free space between the battery and PCB, shown in Figure 6.3. The S22 in this case are plotted together and compared with the desired one in Figure 6.2. In this placement, the diversity antenna has improved a little bit, the additional resonant frequency, which is not expected, disappears. However the return loss is still quite high and do not cover the requirement the frequency bandwidth.

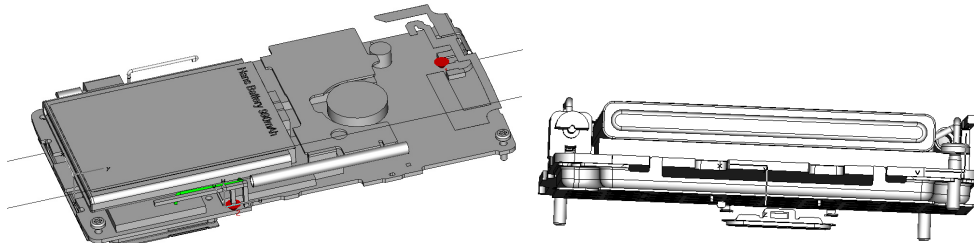


Figure 6.3 Geometry of case 1. (a) view from the top. (b) view from the bottom.

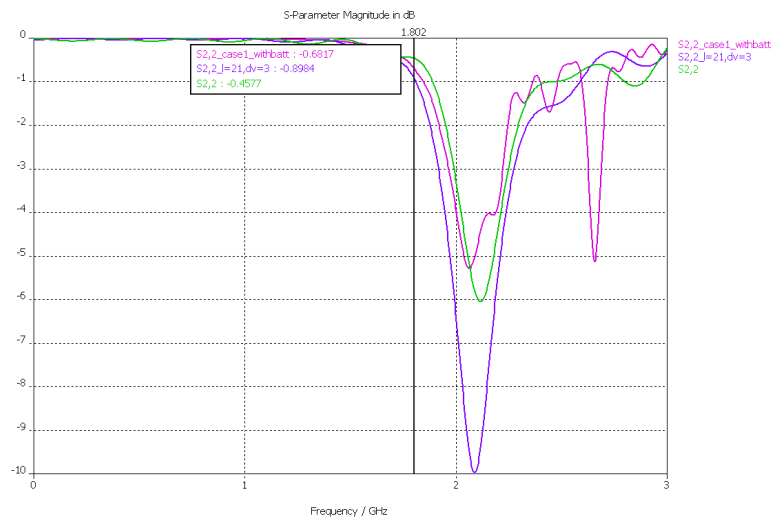


Figure 6.4 Comparison of S22 among case 1, case 2 and the desired case.

### Case 3.

The battery is fully grounded on the PCB, and the antenna is on the edge of left side, and near from the original high band antenna, as shown in Figure 6.5. In this case, the additional resonant frequency disappears, but the return loss is still quite high and do not cover the requirement the frequency bandwidth, shown in Figure 6.6.

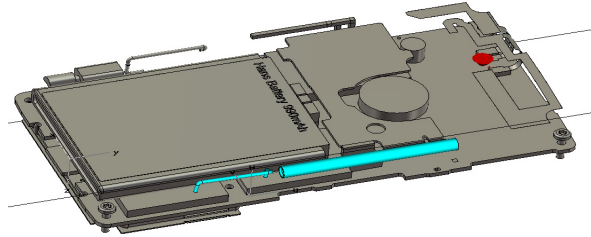


Figure 6.5 Geometry of case 3.

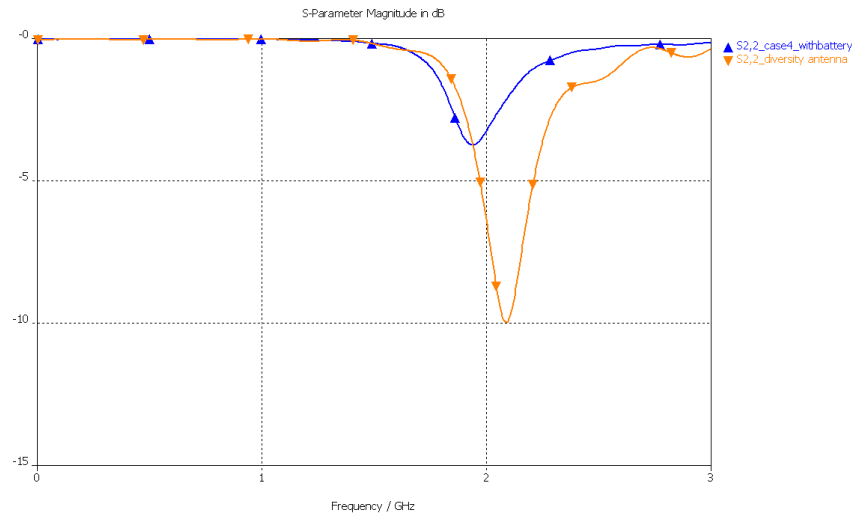


Figure 6.6 Comparison of S22 between case 3 and the desired case.

### Case 4.

The battery placement is the same as case 1, grounded on the PCB but not fully, and the antenna is moved 40mm far away from battery, but near from the original low band antenna, as shown in Figure 6.7. In this case, the diversity antenna and the main antenna are located very close from each other, hence the mutual coupling between these two antennas increase compared with the desired case. Furthermore another resonant frequency occurs, shown in the Figure 6.8.

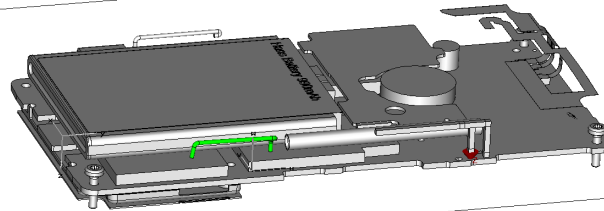


Figure 6.7 Geometry of case 4.

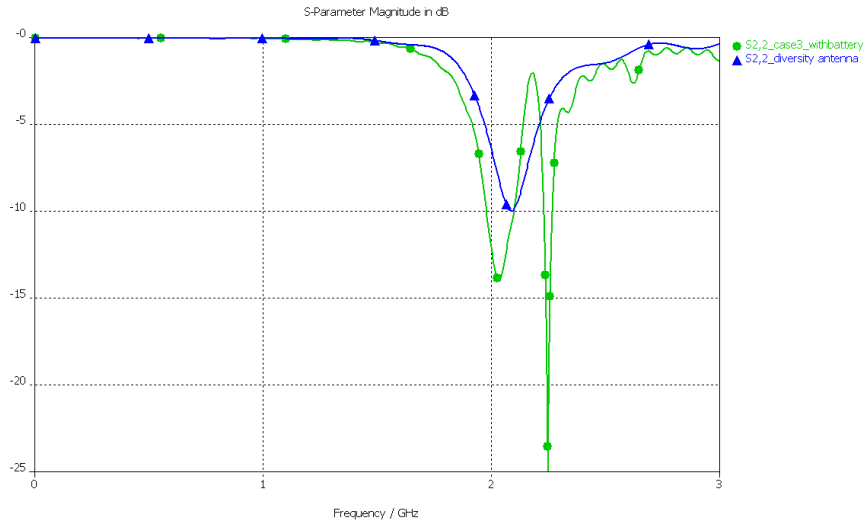


Figure 6.8 Comparison of S22 between case 4 and the desired case.

### 6.3 Available Cases of Placements

#### Case 5.

The geometry in this case is the same as shown in Figure 6.7, but the battery is fully grounded on the PCB. Figure 6.9 shows the reflection coefficient of main antenna and diversity antenna, also compared with that of the original main antenna. The reflection coefficient of the main antenna changes slightly when the diversity antenna is implemented in this case. The diversity antenna has low return loss at the resonant frequency, although another resonant frequency exists at about 2.7 GHz, which is acceptable, since the return loss is very high at this frequency.

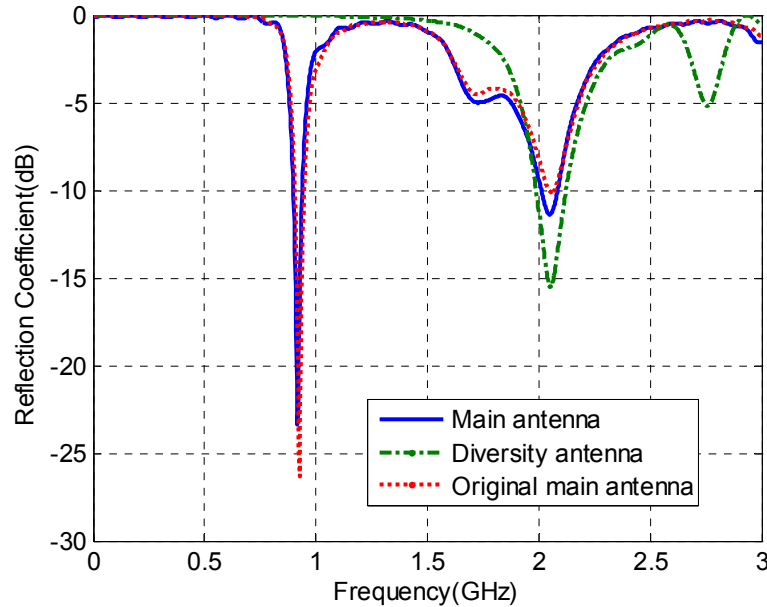


Figure 6.9 Comparison of reflection coefficient.

In this case, correlation coefficient, which is calculated from far-field function in the simulation, between the main and diversity antennas is 0.03. Consequently, 9.99dB

apparent diversity gain is obtained. The stronger efficiency of these two antennas is 0.90, thus the effective diversity gain in this case is 9.54 dB.

### Case 6.

The diversity antenna is located at the bottom of the mobile terminal, and is rotated outside about 7 degrees, shown in Figure 6.10. Figure 6.11 shows the reflection coefficient of main antenna and diversity antenna, also compared with that of the original main antenna. For the diversity antenna, there is no another resonant frequency, compared with case 5. After simulation and calculation, 0.17 correlation coefficient is obtained in this case. When the stronger efficiency is taken into account, 9.94 dB apparent diversity gain and 9.23 dB effective diversity gain are obtained.

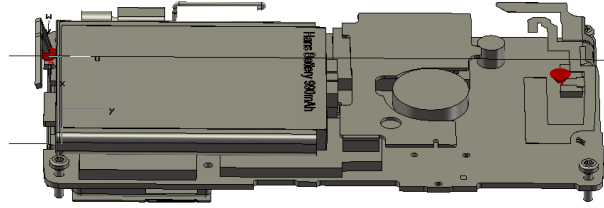


Figure 6.10 Geometry of case 6.

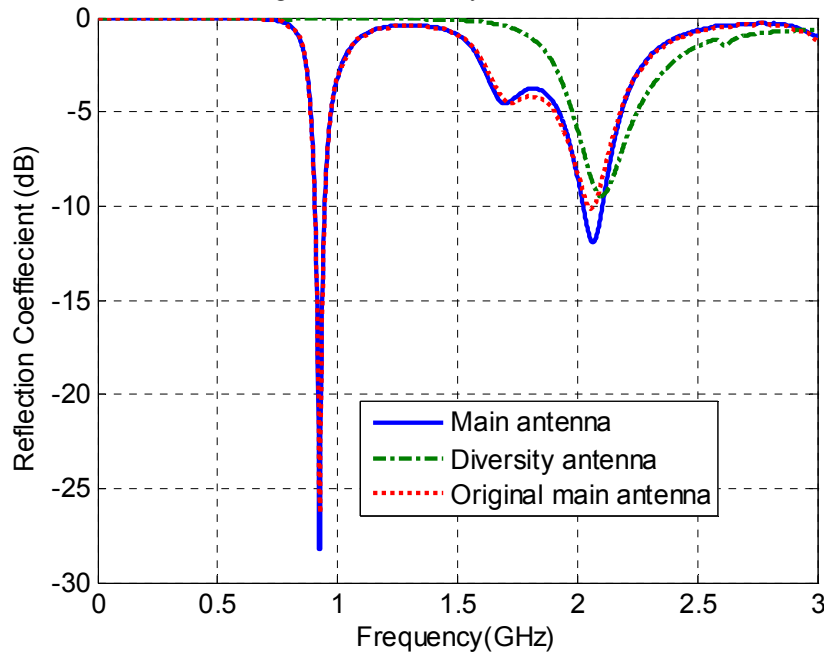


Figure 6.11 Comparison of reflection coefficient

### Case 7.

The diversity antenna is located under the low band part of the original antenna, shown in Figure 6.12. From Figure 6.13, we can see that both main antenna and diversity antenna have low return loss at high frequency band. However the existence of the diversity antenna has obvious impact on the low band part of the original antenna due to the high mutual coupling between them. Furthermore, the resonant frequency is decreased, but it can be solved by changing the dimension of the antennas. In this case, the correlation coefficient from far-field function is 0.33, calculated apparent diversity gain and effective diversity gain are 9.75 dB and 8.07 dB, respectively.

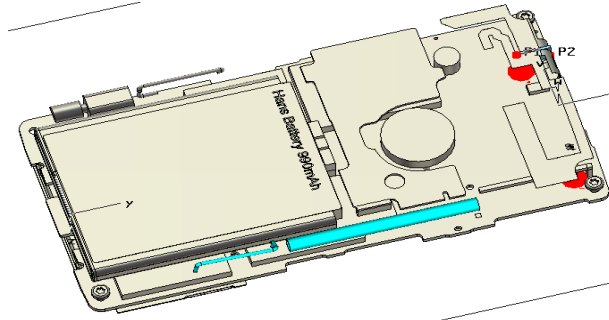


Figure 6.12 Geometry of case 7

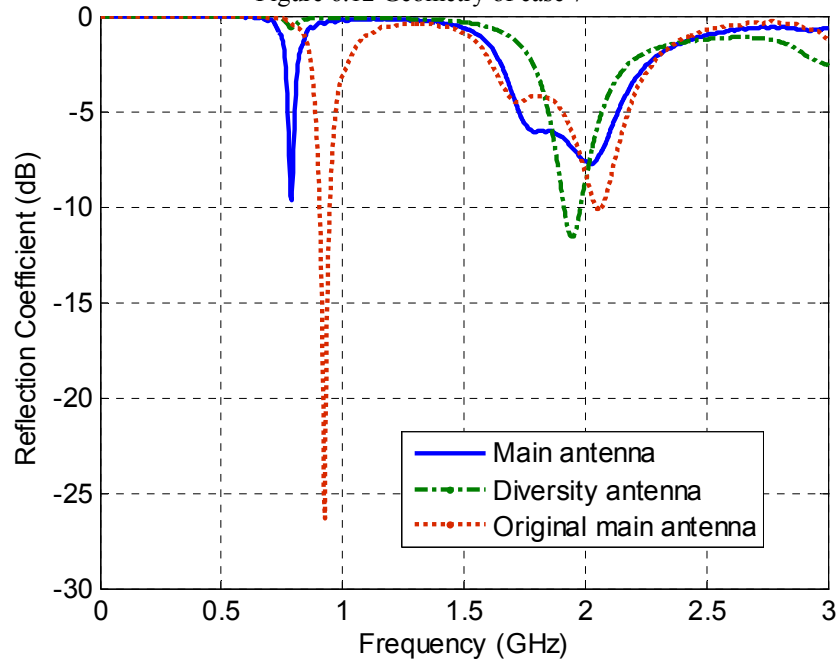


Figure 6.13 Comparison of reflection coefficient

## 6.4 Conclusion

It is difficult to put a diversity antenna inside an existing mobile terminal, since there is no sufficient space to accommodate it. Several trials have been done in the simulations to find a proper placement of the diversity antenna, but only some of them are presented here. Through these cases, we can see some common conclusions. The battery has the most important effect on the diversity antenna performance, since the diversity antenna is most likely to be close to the battery. Furthermore, the diversity antenna has better performance if the battery is fully grounded on the PCB. However, in some locations, both main antenna and diversity antenna have good performance, low correlation and high diversity gain can be obtained.

## 7. Summary, Discussion and Future Work

Diversity is a large, promising and integrated topic in the new generation of wireless communication system. With diversity, the fading problems can be overcome, and furthermore better signal performance can be obtained, both in high data rate and low error rate. Diversity involves many areas, not only antennas but also switch combiner, filter, etc. Therefore it is difficult to study diversity systematically in such a five month's master thesis. The main focus of this work is on the diversity performance from the point of view of antennas.

In this work, studies and evaluations have confirmed that the correlation coefficients calculated from far-field functions and S parameters are equivalent in an antenna system, assuming uniform distributed propagation model is used. Since the focus of the study is diversity gain of a diversity antenna system, we have performed three stages to study the diversity gain step by step. In the first stage, two half wave dipoles have been studied. The diversity algorithm is evaluated and verified, comparing with previous papers. In the second stage, the study of diversity gain obtained with two PIFA antennas on a small ground plane is performed, both in simulation and measurement. Correlation coefficient, diversity gain against the distance between these two PIFA antennas are studied, low correlation coefficient and high effective diversity gain are obtained. Furthermore we can benefit from matching networks on diversity performance. After matching networks, lower correlation coefficient is definitely obtained. However the effective diversity gain, which is more important in an antenna diversity system, depends not only on low correlation coefficient but also on high embedded element efficiency. Therefore it is really important to find the balance between the correlation coefficient and efficiency when design the matching networks. In the third stage, the antenna diversity performance has been studied in full phone case. Different placements of the diversity antenna show the different results of antenna performance of both the main antenna and the diversity antenna. Based on the resonant frequency and bandwidth requirements, some placements of the diversity match the requirements and obtain low correlation coefficient and high diversity gain.

It is worth to note that the settings in the CST MicroWave Studio is very important when calculating in the MPA, since the imported files are from CST MicroWave Studio in this work, refer to APPENDIX . The embedded element efficiency calculated in MPA is quite different when the integration step is changed from 1 degree to 15 degrees.

About the future work, we can continue the diversity study in full phone case and to evaluate the diversity gain against different antenna placements and compare simulations with measurements; we can also do the simulations with hand and head phantom to study the effect from operator tissues on the diversity performance. Furthermore, different environment parameters is another interest to study the diversity performance considering different propagation models.

## Reference

- [1] R. G. Vaughan and J. Bach Andersen, "Antenna diversity in mobile communications," *IEEE Trans. Veh. Technol.*, vol. VT-36, Nov. 1987.
- [2] P.-S. Kildal and K. Rosengren, "Correlation and capacity of MIMO systems and mutual coupling, radiation efficiency and diversity gain of their antennas: Simulations and measurements in reverberation chamber", *IEEE Communications Magazine*, vol. 42, no.12, pp. 102-112, Dec. 2004.'
- [3] P-S. Kildal, K. Rosengren, J. Byun and J. Lee, "Definition of effective diversity gain and how measure it in a reverberation chamber", *Microwave and Optical Technology Letters*, vol. 34, No 1, pp. 56-59, July, 2002.
- [4] Kristian Karlsson, Jan Carlsson, Ilja Belov, Göran Nilsson, P.-S. Kildal, "Optimization of Antenna Diversity Gain by Combining Full-Wave and Circuit Simulations". EuCAP 2007, Nov. 11-16, 2007, EICC, Edinburgh, UK.
- [5] T. S. Rappaport, "Wireless Communications, Principles and Practice", Pearson Education.
- [6] K. Fijimoto, J. R. James, "Mobile Antenna System Handbook", Artech House, 2000.
- [7] M. Schwartz, W. R. Bennett, S. Stein, "Communication System and Techniques", New York, McGraw-Hill, 1965
- [8] Kent, Rosengren, "Characterization of Terminal Antennas for Diversity and MIMO Systems by Theory, Simulations and Measurements in Reverberation Chamber", Ph.D. thesis 2005.
- [9] P-S. Kildal, Kent Rosengren, "Electromagnetic Analysis of Effective and Apparent Diversity Gain of Two Parallel Dipoles", *IEEE antennas and wireless Propagation Letters*, Vol.2. 2003.
- [10] S. Blanch, J. Romeu and I. Corbella, "Exact representation of antenna system diversity performance from input parameter description", *ELECTRONICS LETTERS* 1st May 2003 Vol. 39 No. 9, page 705-707
- [11] Kent Rosengren, P-S. Kildal, "Radiation efficiency, correlation, diversity gain and capacity of a six monopole antenna array for a MIMO system: Theory, Simulation and Measurement in Reverberation Chamber." *Proceedings IEE, Microwaves, Optics and Antennas*, pp. 7-16, Vol. 152, No. 1, Feb. 2005.
- [12] Zhi Ning Chen , "Antenna for Portable Devices", Wiley, 2007.
- [13] Guillermo. Gonzalez, "Microwave Transistor Amplifiers, Analysis and Design ", Prentice Hall, 1997.
- [14] Robert E. Collin, "Foundations for Microwave Engineering", New York, McGraw Hill, 1992.
- [15] MPA short course, Chalmers, 10th, Oct, 2007.
- [17] P.-S. Kildal, "Foundations of antennas - A Unified Approach", textbook from Studentlitteratur, Sweden, 2000.
- [18] Lennart Råde, Bertil Westergren, "BETA, Mathematics Handbook", Studentlitteratur, Lund, Sweden.



## Appendix A

### The Marcum Q-function

Basic definitions and elementary properties [7]:

$$Q(a, b) = \int_b^{\infty} \exp\left(-\frac{a^2 + b^2}{2}\right) I_0(ax) x dx$$

$$Q(\sqrt{2a}, \sqrt{2b}) = \int_b^{\infty} \exp[-(a + y)] I_0(2\sqrt{ay}) dy$$

$$Q(0, b) = \exp\left(-\frac{b^2}{2}\right)$$

$$Q(a, 0) = 1$$

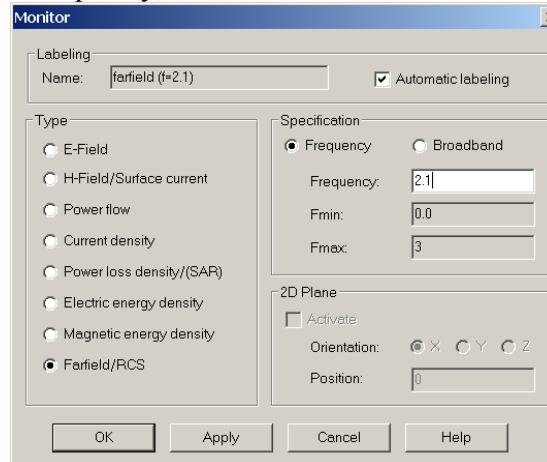
Where  $I_0$  is the modified Bessel function of zeroth order.

## Appendix B

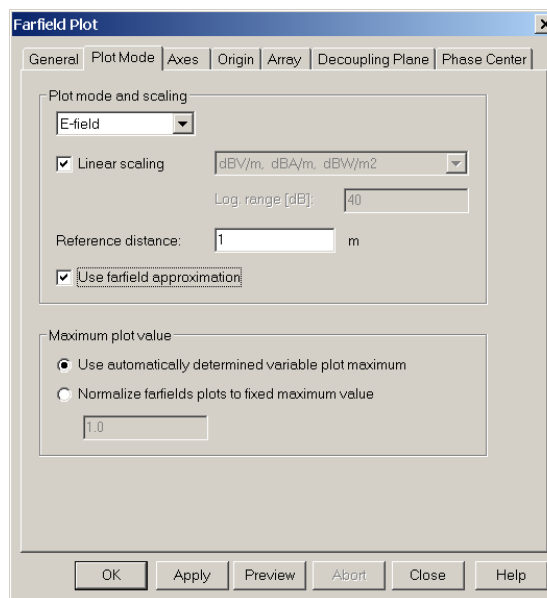
### Settings in CST MicroWave Studio

To properly prepare output data (embedded element patterns and S-parameters) in CST to do the calculation, following steps should be followed:

Radiation pattern: In the far-field monitor: check “Farfield/RCS”, and the change the frequency to the desired frequency, 2.1 GHz in this work.



After simulation, right click "Farfields", under “Plot properties” / “Plot mode”: Select: “E-field” + “linear scaling” and “reference distance” = 1m. (This will make it possible to export the complex (amplitude and phase) far field in unit [V/m]). Also check “Use farfield approximation”:



"General" in "Farfield plot", the angle step can be changed. It will not affect the efficiency calculation in CST, however it will affect not only the accuracy when calculating the correlation coefficient but also the efficiency calculation in MPA.

